

1 Meta-analysis of 375,000 individuals identifies 38 susceptibility 2 loci for migraine

3
4 Padhraig Gormley^{*1,2,3,4}, Verneri Anttila^{*2,3,5}, Bendik S Winsvold^{6,7,8}, Priit Palta⁹, Tonu Esko^{2,10,11}, Tune H.
5 Pers^{2,11,12,13}, Kai-How Farh^{2,5,14}, Ester Cuenca-Leon^{1,2,3,15}, Mikko Muona^{9,16,17,18}, Nicholas A Furlotte¹⁹,
6 Tobias Kurth^{20,21}, Andres Ingason²², George McMahon²³, Lannie Ligthart²⁴, Gisela M Terwindt²⁵, Mikko
7 Kallela²⁶, Tobias M Freilinger^{27,28}, Caroline Ran²⁹, Scott G Gordon³⁰, Anine H Stam²⁵, Stacy Steinberg²²,
8 Guntram Borck³¹, Markku Koiranen³², Lydia Quaye³³, Hieab HH Adams^{34,35}, Terho Lehtimäki³⁶, Antti-
9 Pekka Sarin⁹, Juho Wedenoja³⁷, David A Hinds¹⁹, Julie E Buring^{21,38}, Markus Schürks³⁹, Paul M Ridker^{21,38},
10 Maria Gudlaug Hrafnisdottir⁴⁰, Hreinn Stefansson²², Susan M Ring²³, Jouke-Jan Hottenga²⁴, Brenda WJH
11 Penninx⁴¹, Markus Färkkilä²⁶, Ville Artto²⁶, Mari Kaunisto⁹, Salli Vepsäläinen²⁶, Rainer Malik²⁷, Andrew C
12 Heath⁴², Pamela A F Madden⁴², Nicholas G Martin³⁰, Grant W Montgomery³⁰, Mitja Kurki^{1,2,3}, Mart Kals¹⁰,
13 Reedik Mägi¹⁰, Kalle Pärn¹⁰, Eija Hämäläinen⁹, Hailiang Huang^{2,3,5}, Andrea E Byrnes^{2,3,5}, Lude Franke⁴³, Jie
14 Huang⁴, Evie Stergiakouli²³, Phil H Lee^{1,2,3}, Cynthia Sandor⁴⁴, Caleb Webber⁴⁴, Zameel Cader^{45,46}, Bertram
15 Muller-Myhsok⁴⁷, Stefan Schreiber⁴⁸, Thomas Meitinger⁴⁹, Johan G Eriksson^{50,51}, Veikko Salomaa⁵¹, Kauko
16 Heikkilä⁵², Elizabeth Loehrer^{34,53}, Andre G Uitterlinden⁵⁴, Albert Hofman³⁴, Cornelia M van Duijn³⁴, Lynn
17 Cherkas³³, Linda M. Pedersen⁶, Audun Stubhaug^{55,56}, Christopher S Nielsen^{55,57}, Minna Männikkö³², Evelin
18 Mihailov¹⁰, Lili Milani¹⁰, Hartmut Göbel⁵⁸, Ann-Louise Esserlind⁵⁹, Anne Francke Christensen⁵⁹, Thomas
19 Folkmann Hansen⁶⁰, Thomas Werge^{61,62,63}, International Headache Genetics Consortium⁶⁴, Jaakko
20 Kaprio^{9,65,66}, Arpo J Aromaa⁵¹, Olli Raitakari^{67,68}, M Arfan Ikram^{34,35,68}, Tim Spector³³, Marjo-Riitta
21 Järvelin^{32,70,71,72}, Andres Metspalu¹⁰, Christian Kubisch⁷³, David P Strachan⁷⁴, Michel D Ferrari²⁵, Andrea C
22 Belin²⁹, Martin Dichgans^{27,75}, Maija Wessman^{9,16}, Arn MJM van den Maagdenberg^{25,76}, John-Anker
23 Zwart^{6,7,8}, Dorret I Boomsma²⁴, George Davey Smith²³, Kari Stefansson^{22,77}, Nicholas Eriksson¹⁹, Mark J
24 Daly^{2,3,5}, Benjamin M Neale^{§,2,3,5}, Jes Olesen^{§,59}, Daniel I Chasman^{§,21,38}, Dale R Nyholt^{§,78}, and Aarno
25 Palotie^{§,1,2,3,4,5,9,79}.

26
27 ¹Psychiatric and Neurodevelopmental Genetics Unit, Massachusetts General Hospital and Harvard Medical School, Boston, USA.
28 ²Medical and Population Genetics Program, Broad Institute of MIT and Harvard, Cambridge, USA. ³Stanley Center for Psychiatric
29 Research, Broad Institute of MIT and Harvard, Cambridge, USA. ⁴Wellcome Trust Sanger Institute, Wellcome Trust Genome
30 Campus, Hinxton, UK. ⁵Analytic and Translational Genetics Unit, Massachusetts General Hospital and Harvard Medical School,
31 Boston, USA. ⁶FORMI, Oslo University Hospital, P.O. 4956 Nydalen, 0424 Oslo, Norway. ⁷Department of Neurology, Oslo
32 University Hospital, P.O. 4956 Nydalen, 0424 Oslo, Norway. ⁸Institute of Clinical Medicine, University of Oslo, P.O. 1171
33 Blindern, 0318 Oslo, Norway. ⁹Institute for Molecular Medicine Finland (FIMM), University of Helsinki, Helsinki, Finland.
34 ¹⁰Estonian Genome Center, University of Tartu, Tartu, Estonia. ¹¹Division of Endocrinology, Boston Children's Hospital, Boston,
35 USA. ¹²Statens Serum Institut, Dept of Epidemiology Research, Copenhagen, Denmark. ¹³Novo Nordisk Foundation Center for
36 Basic Metabolic Research, University of Copenhagen, Copenhagen, Denmark. ¹⁴Illumina, 5200 Illumina Way, San Diego, USA.
37 ¹⁵Vall d'Hebron Research Institute, Pediatric Neurology, Barcelona, Spain. ¹⁶Folkhälsan Institute of Genetics, Helsinki, Finland,
38 FI-00290. ¹⁷Neuroscience Center, University of Helsinki, Helsinki, Finland, FI-00014. ¹⁸Research Programs Unit, Molecular
39 Neurology, University of Helsinki, Helsinki, Finland, FI-00014. ¹⁹23andMe, Inc., 899 W. Evelyn Avenue, Mountain View, CA, USA.
40 ²⁰Inserm Research Center for Epidemiology and Biostatistics (U897), University of Bordeaux, 33076 Bordeaux, France. ²¹Division
41 of Preventive Medicine, Brigham and Women's Hospital, Boston MA 02215. ²²deCODE Genetics, 101 Reykjavik, Iceland.
42 ²³Medical Research Council (MRC) Integrative Epidemiology Unit, University of Bristol, Bristol, UK. ²⁴VU University Amsterdam,
43 Department of Biological Psychology, Amsterdam, the Netherlands, 1081 BT. ²⁵Leiden University Medical Centre, Department

44 of Neurology, Leiden, The Netherlands, PO Box 9600, 2300 RC. ²⁶Department of Neurology, Helsinki University Central Hospital,
45 Haartmaninkatu 4, 00290 Helsinki, Finland. ²⁷Institute for Stroke and Dementia Research, Klinikum der Universität München,
46 Ludwig-Maximilians-Universität München, Feodor-Lynen-Str. 17, 81377 Munich Germany. ²⁸Department of Neurology and
47 Epileptology, Hertie Institute for Clinical Brain Research, University of Tuebingen. ²⁹Karolinska Institutet, Department of
48 Neuroscience, 171 77 Stockholm, Sweden. ³⁰Department of Genetics and Computational Biology, QIMR Berghofer Medical
49 Research Institute, 300 Herston Road, Brisbane, QLD 4006, Australia. ³¹Ulm University, Institute of Human Genetics, 89081 Ulm,
50 Germany. ³²University of Oulu, Center for Life Course Epidemiology and Systems Medicine, Oulu, Finland, Box 5000, Fin-90014
51 University of Oulu. ³³Department of Twin Research and Genetic Epidemiology, King's College London, London, UK. ³⁴Dept of
52 Epidemiology, Erasmus University Medical Center, Rotterdam, the Netherlands, 3015 CN. ³⁵Dept of Radiology, Erasmus
53 University Medical Center, Rotterdam, the Netherlands, 3015 CN. ³⁶Department of Clinical Chemistry, Fimlab Laboratories, and
54 School of Medicine, University of Tampere, Tampere, Finland, 33520. ³⁷Department of Public Health, University of Helsinki,
55 Helsinki, Finland. ³⁸Harvard Medical School, Boston MA 02115. ³⁹University Duisburg Essen, Essen, Germany. ⁴⁰Landspítali
56 University Hospital, 101 Reykjavik, Iceland. ⁴¹VU University Medical Centre, Department of Psychiatry, Amsterdam, the
57 Netherlands, 1081 HL. ⁴²Department of Psychiatry, Washington University School of Medicine, 660 South Euclid, CB 8134, St.
58 Louis, MO 63110, USA. ⁴³University Medical Center Groningen, University of Groningen, Groningen, The Netherlands, 9700RB.
59 ⁴⁴MRC Functional Genomics Unit, Department of Physiology, Anatomy & Genetics, Oxford University, UK. ⁴⁵Nuffield
60 Department of Clinical Neuroscience, University of Oxford, UK. ⁴⁶Oxford Headache Centre, John Radcliffe Hospital, Oxford, UK.
61 ⁴⁷Max-Planck-Institute of Psychiatry, Munich, Germany. ⁴⁸Christian Albrechts University, Kiel, Germany. ⁴⁹Institute of Human
62 Genetics, Helmholtz Center Munich, Neuherberg, Germany. ⁵⁰Department of General Practice and Primary Health Care,
63 University of Helsinki and Helsinki University Hospital, Helsinki Finland. ⁵¹National Institute for Health and Welfare, Helsinki,
64 Finland. ⁵²Institute of Clinical Medicine, University of Helsinki, Helsinki, Finland. ⁵³Department of Environmental Health, Harvard
65 T.H. Chan School of Public Health, Boston, USA 02115. ⁵⁴Dept of Internal Medicine, Erasmus University Medical Center,
66 Rotterdam, the Netherlands, 3015 CN. ⁵⁵Dept of Pain Management and Research, Oslo University Hospital, Oslo, 0424 Oslo,
67 Norway. ⁵⁶Medical Faculty, University of Oslo, Oslo, 0318 Oslo, Norway. ⁵⁷Division of Mental Health, Norwegian Institute of
68 Public Health, P.O. Box 4404 Nydalen, Oslo, Norway, NO-0403. ⁵⁸Kiel Pain and Headache Center, 24149 Kiel, Germany. ⁵⁹Danish
69 Headache Center, Department of Neurology, Rigshospitalet, Glostrup Hospital, University of Copenhagen, Denmark. ⁶⁰Institute
70 of Biological Psychiatry, Mental Health Center Sct. Hans, University of Copenhagen, Roskilde, Denmark. ⁶¹Institute Of Biological
71 Psychiatry, MHC Sct. Hans, Mental Health Services Copenhagen, DK-2100 Copenhagen, Denmark. ⁶²Institute of Clinical Sciences,
72 Faculty of Medicine and Health Sciences, University of Copenhagen, DK-2100 Copenhagen, Denmark. ⁶³PSYCH - The Lundbeck
73 Foundation's Initiative for Integrative Psychiatric Research, DK-2100 Copenhagen, Denmark. ⁶⁴A list of members and affiliations
74 appears in the Supplementary Note. ⁶⁵Department of Public Health, University of Helsinki, Helsinki, Finland. ⁶⁶Department of
75 Health, National Institute for Health and Welfare, Helsinki, Finland. ⁶⁷Research Centre of Applied and Preventive Cardiovascular
76 Medicine, University of Turku, Turku, Finland, 20521. ⁶⁸Department of Clinical Physiology and Nuclear Medicine, Turku
77 University Hospital, Turku, Finland, 20521. ⁶⁹Dept of Neurology, Erasmus University Medical Center, Rotterdam, the
78 Netherlands, 3015 CN. ⁷⁰Imperial College London, Department of Epidemiology and Biostatistics, MRC Health Protection Agency
79 (HPE) Centre for Environment and Health, School of Public Health, UK, W2 1PG. ⁷¹University of Oulu, Biocenter Oulu, Finland,
80 Box 5000, Fin-90014 University of Oulu. ⁷²Oulu University Hospital, Unit of Primary Care, Oulu, Finland, Box 10, Fin-90029 OYS.
81 ⁷³University Medical Center Hamburg Eppendorf, Institute of Human Genetics, 20246 Hamburg, Germany. ⁷⁴Population Health
82 Research Institute, St George's, University of London, Cranmer Terrace, London SW17 0RE, UK. ⁷⁵Munich Cluster for Systems
83 Neurology (SyNergy), Munich, Germany. ⁷⁶Leiden University Medical Centre, Department of Human Genetics, Leiden, The
84 Netherlands, PO Box 9600, 2300 RC. ⁷⁷Faculty of Medicine, University of Iceland, 101 Reykjavik, Iceland. ⁷⁸Statistical and
85 Genomic Epidemiology Laboratory, Institute of Health and Biomedical Innovation, Queensland University of Technology, 60
86 Musk Ave, Kelvin Grove, QLD 4059, Australia. ⁷⁹Department of Neurology, Massachusetts General Hospital, Boston, USA.

87
88 * These authors contributed equally to this work.

89 [§] These authors jointly supervised this work.

90
91 Correspondence should be addressed to Aarno Palotie (aarno.palotie@helsinki.fi).

92 **Migraine is a debilitating neurological disorder affecting around 1 in 7 people worldwide,**
93 **but its molecular mechanisms remain poorly understood. Some debate exists over**
94 **whether migraine is a disease of vascular dysfunction or a result of neuronal dysfunction**
95 **with secondary vascular changes. Genome-wide association (GWA) studies have thus far**
96 **identified 13 independent loci associated with migraine. To identify new susceptibility**
97 **loci, we performed the largest genetic study of migraine to date, comprising 59,674 cases**
98 **and 316,078 controls from 22 GWA studies. We identified 44 independent single**
99 **nucleotide polymorphisms (SNPs) significantly associated with migraine risk ($P < 5 \times 10^{-8}$)**
100 **that map to 38 distinct genomic loci, including 28 loci not previously reported and the**
101 **first locus identified on chromosome X. In subsequent computational analyses, the**
102 **identified loci showed enrichment for genes expressed in vascular and smooth muscle**
103 **tissues, consistent with a predominant theory of migraine that highlights vascular**
104 **etiologies.**

105
106 Migraine is ranked as the third most common disease worldwide, with a lifetime prevalence of
107 15-20%, affecting up to one billion people across the globe^{1,2}. It ranks as the 7th most disabling
108 of all diseases worldwide (or 1st most disabling neurological disease) in terms of years of life lost
109 to disability¹ and is the 3rd most costly neurological disorder after dementia and stroke³. There is
110 debate about whether migraine is a disease of vascular dysfunction, or a result of neuronal
111 dysfunction with vascular changes representing downstream effects not themselves causative
112 of migraine^{4,5}. However, genetic evidence favoring one theory versus the other is lacking. At the
113 phenotypic level, migraine is defined by diagnostic criteria from the International Headache
114 Society⁶. There are two prevalent sub-forms: migraine without aura is characterized by recurrent
115 attacks of moderate or severe headache associated with nausea or hypersensitivity to light and
116 sound. Migraine with aura is characterized by transient visual and/or sensory and/or speech
117 symptoms usually followed by a headache phase similar to migraine without aura.

118
119 Family and twin studies estimate a heritability of 42% (95% confidence interval [CI] = 36-47%)
120 for migraine⁷, pointing to a genetic component of the disease. Despite this, genetic association
121 studies have revealed relatively little about the molecular mechanisms that contribute to
122 pathophysiology. Understanding has been limited partly because, to date, only 13 genome-wide
123 significant risk loci have been identified for the prevalent forms of migraine⁸⁻¹¹. In familial
124 hemiplegic migraine (FHM), a rare Mendelian form of the disease, three ion transport-related
125 genes (*CACNA1A*, *ATP1A2* and *SCN1A*) have been implicated¹²⁻¹⁴. These findings suggest that

126 mechanisms that regulate neuronal ion homeostasis might also be involved in migraine more
127 generally, however, no genes related to ion transport have yet been identified for these more
128 prevalent forms of migraine¹⁵.

129

130 We performed a meta-analysis of 22 genome-wide association (GWA) studies, consisting of
131 59,674 cases and 316,078 controls collected from six tertiary headache clinics and 27
132 population-based cohorts through our worldwide collaboration in the International Headache
133 Genetics Consortium (IHGC). This combined dataset contained over 35,000 new migraine
134 cases not included in previously published GWA studies. Here we present the findings of this
135 new meta-analysis, including 38 genomic loci, harboring 44 independent association signals
136 identified at levels of genome-wide significance, which support current theories of migraine
137 pathophysiology and also offer new insights into the disease.

138

139 Results

140 Significant associations at 38 independent genomic loci

141 The primary meta-analysis was performed on all migraine samples available through the IHGC,
142 regardless of ascertainment. These case samples included both individuals diagnosed with
143 migraine by a doctor as well as individuals with self-reported migraine via questionnaires. Study
144 design and sample ascertainment for each individual study is outlined in the **Supplementary**
145 **Note** (and summarized in **Supplementary Table 1**). The final combined sample consisted of
146 59,674 cases and 316,078 controls in 22 non-overlapping case-control samples (**Table 1**). All
147 samples were of European ancestry. Before including the largest study from 23andMe, we
148 confirmed that it did not contribute any additional heterogeneity compared to the other
149 population and clinic-based studies (**Supplementary Table 2**).

150

151 The 22 individual GWA studies completed standard quality control protocols (**Online Methods**)
152 summarized in **Supplementary Table 3**. Missing genotypes were then imputed into each
153 sample using a common 1000 Genomes Project reference panel¹⁶. Association analyses were
154 performed within each study using logistic regression on the imputed marker dosages while
155 adjusting for sex and other covariates where necessary (**Online Methods** and **Supplementary**
156 **Table 4**). The association results were combined using an inverse-variance weighted fixed-
157 effects meta-analysis. Markers were filtered for imputation quality and other metrics (**Online**
158 **Methods**) leaving 8,094,889 variants for consideration in our primary analysis.

159

160 Among these variants in the primary analysis, we identified 44 genome-wide significant SNP
161 associations ($P < 5 \times 10^{-8}$) that are independent ($r^2 < 0.1$) with regards to linkage disequilibrium
162 (LD). We validated the 44 SNPs by comparing genotypes in a subset of the sample to those
163 obtained from whole-genome sequencing (**Supplementary Table 5**). To help identify candidate
164 risk genes from these, we defined an associated locus as the genomic region bounded by all
165 markers in LD ($r^2 > 0.6$ in 1000 Genomes, Phase I, EUR individuals) with each of the 44 index
166 SNPs and in addition, all such regions in close proximity (< 250 kb) were merged. From these
167 defined regions we implicate 38 distinct genomic loci in total for the prevalent forms of migraine,
168 28 of which have not previously been reported (**Figure 1**).

169

170 These 38 loci replicate 10 of the 13 previously reported genome-wide associations to migraine
171 (**Table 2**). Six of the 38 loci contain a secondary genome-wide significant SNP ($P < 5 \times 10^{-8}$) not
172 in LD ($r^2 < 0.1$) with the top SNP in the locus (**Table 2**). Five of these secondary signals were
173 found in known loci (at *LRP1*, *PRDM16*, *FHL5*, *TRPM8*, and *TSPAN2*), while the sixth was
174 found within one of the 28 new loci (*PLCE1*). Therefore, out of the 44 LD-independent SNPs
175 reported here, 34 are new associations to migraine. Three previously reported loci that were
176 associated to subtypes of migraine (rs1835740 near *MTDH* to migraine with aura, rs10915437
177 near *AJAP1* to migraine clinical-samples, and rs10504861 near *MMP16* to migraine without
178 aura)^{8,11} show only nominal significance in the current meta-analysis ($P = 5 \times 10^{-3}$ for
179 rs1835740, $P = 4.4 \times 10^{-5}$ for rs10915437, and $P = 4.9 \times 10^{-5}$ for rs10504861, **Supplementary**
180 **Table 6**), however, these loci have since been shown to be associated to specific phenotypic
181 features of migraine¹⁷ and therefore may require a more phenotypically homogeneous sample
182 to be accurately assessed for association. Four out of 44 SNPs (at *TRPM8*, *ZCCHC14*, *MRVI1*,
183 and *CCM2L*) exhibited moderate heterogeneity across the individual GWA studies (Cochran's Q
184 test p -value < 0.05 , **Supplementary Table 7**) therefore at these markers we applied a random
185 effects model¹⁸.

186

187 Characterization of the associated loci

188 In total, 32 of 38 (84%) loci overlap with transcripts from protein-coding genes, and 17 (45%) of
189 these regions contain just a single gene (see **Supplementary Figure 1** for regional plots of the
190 38 genomic loci and **Supplementary Table 8** for extended information on each locus). Among
191 the 38 loci, only two contain ion channel genes (*KCNK5*¹⁹ and *TRPM8*²⁰). Hence, despite
192 previous hypotheses of migraine as a potential channelopathy^{5,21}, the loci identified to date do

193 not support common variants in ion channel genes as strong susceptibility components in
194 prevalent forms of migraine. However, three other loci do contain genes involved more generally
195 in ion homeostasis (*SLC24A3*²², *ITPK1*²³, and *GJA1*²⁴, **Supplementary Table 9**).

196

197 Several of the genes have previous associations to vascular disease (*PHACTR1*,^{25,26}
198 *TGFBR2*,²⁷ *LRP1*,²⁸ *PRDM16*,²⁹ *RNF213*,³⁰ *JAG1*,³¹ *HEY2*,³² *GJA1*³³, *ARMS2*³⁴), or are
199 involved in smooth muscle contractility and regulation of vascular tone (*MRVI1*,³⁵ *GJA1*,³⁶
200 *SLC24A3*,³⁷ *NRP1*³⁸). Three of the 44 migraine index SNPs have previously reported
201 associations in the National Human Genome Research Institute (NHGRI) GWAS catalog at
202 exactly the same SNP (rs9349379 at *PHACTR1* with coronary heart disease^{39–41}, coronary
203 artery calcification⁴², and cervical artery dissection; rs11624776 at *ITPK1* with thyroid hormone
204 levels⁴³; and rs11172113 at *LRP1* with pulmonary function; **Supplementary Table 10**). Six of
205 the loci harbor genes that are involved in nitric oxide signaling and oxidative stress (*REST*⁴⁴,
206 *GJA1*⁴⁵, *YAP1*⁴⁶, *PRDM16*⁴⁷, *LRP1*⁴⁸, and *MRVI1*⁴⁹).

207

208 From each locus we chose the nearest gene to the index SNP to assess gene expression
209 activity in tissues from the GTEx consortium (**Supplementary Figure 2**). While we found that
210 most of the putative migraine loci genes were expressed in many different tissue types, we
211 could detect tissue specificity in certain instances whereby some genes showed significantly
212 higher expression in a particular tissue group relative to the others. For instance four genes
213 were more actively expressed in brain (*GPR149*, *CFDP1*, *DOCK4*, and *MPPED2*) compared to
214 other tissues, whereas eight genes were specifically active in vascular tissues (*PRDM16*,
215 *MEF2D*, *FHL5*, *C7orf10*, *YAP1*, *LRP1*, *ZCCHC14*, and *JAG1*). Many of the other putative
216 migraine loci genes were actively expressed in more than one tissue group.

217

218 Genomic inflation and LD-score regression analysis

219 To assess whether the 38 loci harbor true associations with migraine rather than reflecting
220 systematic differences between cases and controls (such as population stratification) we
221 analyzed the genome-wide inflation of test statistics in our primary meta-analysis. As expected
222 for a complex polygenic trait, the distribution of test statistics deviates from the null (genomic
223 inflation factor $\lambda_{GC} = 1.24$, **Supplementary Figure 3**) which is in line with other large GWA study
224 meta-analyses^{50–53}. Since much of the inflation in a polygenic trait arises from LD between the
225 causal SNPs and many other neighboring SNPs in the local region, we LD-pruned the meta-
226 analysis results to create a set of LD-independent markers (i.e. in PLINK⁵⁴ with a 250-kb sliding

227 window and $r^2 > 0.2$). The resulting genomic inflation was reduced ($\lambda_{GC} = 1.15$, **Supplementary**
228 **Figure 4**) and likely reflects the inflation remaining due to the polygenic signal at many
229 independent loci, including those not yet significantly associated.

230
231 To confirm that the observed inflation is primarily coming from true polygenic signal, we
232 analyzed the meta-analysis results from all imputed markers using LD-score regression⁵⁵. This
233 method tests for a linear relationship between marker test statistics and LD score, defined as
234 the sum of r^2 values between a marker and all other markers within a 1-Mb window. The primary
235 analysis results show a linear relationship between association test statistics and LD-score
236 (**Supplementary Figure 5**) and estimate that the majority (88.2%) of the inflation in test
237 statistics can be ascribed to true polygenic signal rather than population stratification or other
238 confounders. These results are consistent with the theory of polygenic disease architecture
239 shown previously by both simulation and real data for GWAS samples of similar size⁵⁶.

240

241 Migraine subtype analyses

242 To elucidate pathophysiological mechanisms underpinning the migraine aura, we performed a
243 secondary analysis by creating two subsets that included only samples with the subtypes;
244 migraine with aura and migraine without aura. These subsets only included those studies where
245 sufficient information was available to assign a diagnosis of either subtype according to
246 classification criteria standardized by the International Headache Society (IHS)⁶. For the
247 population-based study samples this involved questionnaires, whereas for the clinic-based
248 study samples the diagnosis was assigned on the basis of a structured interview by telephone
249 or in person. A stricter diagnosis is required for these migraine subtypes as the migraine aura
250 specifically is challenging to distinguish from other neurological features that can present as
251 symptoms from unrelated conditions.

252

253 As a result, the migraine subtype analyses consisted of considerably smaller sample sizes
254 compared to the main analysis (6,332 cases vs. 144,883 controls for migraine with aura and
255 8,348 cases vs. 139,622 controls for migraine without aura, see **Table 1**). As with the primary
256 migraine analysis, the test statistics for migraine with aura or migraine without aura were
257 consistent with underlying polygenic architecture rather than other potential sources of inflation
258 (**Supplementary Figure 6 and 7**). For the migraine without aura subset analysis we found
259 seven independent genomic loci (near *TSPAN2*, *TRPM8*, *PHACTR1*, *FHL5*, *ASTN2*, near
260 *FGF6*, and *LRP1*) to be significantly associated (**Supplementary Table 11** and **Supplementary**

261 **Figure 8**). All seven of these loci were already identified in the primary analysis of ‘all migraine’
262 types, possibly reflecting the fact that migraine without aura is the most common form of
263 migraine (around 2 in 3 cases) and likely drives the association signals in the primary analysis.
264 Notably, no loci were associated to migraine with aura in the other subset analysis
265 (**Supplementary Figure 9**).

266
267 To investigate whether excess heterogeneity could be contributing to the lack of associations in
268 migraine with aura, we performed a heterogeneity analysis between the two subgroups. First we
269 created two subsets of the migraine with aura and migraine without aura datasets from which
270 none of the case or control individuals were overlapping (**Supplementary Table 12**). Then we
271 selected the 44 LD-independent SNPs associated from the primary analysis and used a
272 random-effects model to combine the migraine with aura and migraine without aura samples in
273 a meta-analysis that allows for heterogeneity between the two migraine groups⁵⁷. We found little
274 heterogeneity with only seven of the 44 SNPs (at *REST*, *MPPED2*, *PHACTR1*, *ASTN2*, *MEF2D*,
275 *PLCE1*, and *MED14*) exhibiting some signs of heterogeneity across subtype groups
276 (**Supplementary Table 13**).

277 278 Credible sets of markers within each locus

279 For each of the 38 migraine-associated loci, we defined a credible set of markers that could
280 plausibly be considered as causal using a Bayesian-likelihood based approach⁵⁸. This method
281 incorporates evidence from association test statistics and the LD structure between SNPs in a
282 locus (**Online Methods**). A list of the credible set SNPs obtained for each locus is provided in
283 **Supplementary Table 14**. We found three instances (in *RNF213*, *PLCE1*, and *MRVI1*) where
284 the association signal could be credibly attributed to exonic missense polymorphisms
285 (**Supplementary Table 15**). However, most of the credible markers at each locus were either
286 intronic or intergenic, which is consistent with the theory that most variants detected by GWA
287 studies involve regulatory effects on gene expression rather than disrupting protein
288 structure^{59,60}.

289 290 Overlap with eQTLs in specific tissues

291 To try to identify specific migraine loci that might influence gene expression, we used previously
292 published datasets that catalog expression quantitative trait loci (eQTLs) in either of two
293 microarray-based studies from peripheral venous blood ($N_1 = 3,754$) or from human brain cortex
294 tissue ($N_2 = 550$). Additionally, we used a third study based on RNAseq data from a collection of

295 42 tissues and three cell lines ($N_3 = 1,641$) from the Genotype-Tissue Expression (GTEx)
296 consortium⁶¹. While this data has the advantage of a diverse tissue catalog, the number of
297 samples per tissue is relatively small (**Supplementary Table 16**) compared to the two
298 microarray datasets, possibly resulting in reduced power to detect significant eQTLs in some
299 tissues. Using these datasets we applied a method based on the overlap of migraine and eQTL
300 credible sets to identify eQTLs that could explain associations at the 38 migraine loci (**Online**
301 **Methods**). This approach merged the migraine credible sets defined above with credible sets
302 from *cis*-eQTL signals within a 1-Mb window and tested if the association signals between the
303 migraine and eQTL credible sets were correlated. After adjusting for multiple testing we found
304 no plausible eQTL associations in the peripheral blood or brain cortex data (**Supplementary**
305 **Tables 17-18 and Supplementary Figure 10**). In GTEx, however, we found evidence for
306 overlap from eQTLs in three tissues (Lung, Tibial Artery, and Aorta) at the *HPSE2* locus and in
307 one tissue (Thyroid) at the *HEY2* locus (**Supplementary Table 19 and Supplementary Figure**
308 **15**).

309
310 In summary, from three datasets we implicate eQTL signals at only two loci (*HPSE2*, and
311 *HEY2*). This low number (two out of 38) is consistent with previous studies which have observed
312 that available eQTL catalogues currently lack sufficient tissue specificity and developmental
313 diversity to provide enough power to provide meaningful biological insight⁵². No plausibly causal
314 eQTLs were observed in expression data from brain.

315

316 Gene expression enrichment in specific tissues

317 To understand if the 38 migraine loci as a group are enriched for expression in certain tissue
318 groups, we again used the GTEx pilot data⁶¹. This time we tested whether genes near to
319 credibly causal SNPs at the 38 migraine loci were significantly enriched for expression in certain
320 tissues (**Online Methods**). We found four tissues that were significantly enriched (after
321 Bonferroni correction) for expression of the migraine genes (**Figure 2**). The two most strongly
322 enriched tissues were part of the cardiovascular system; the *aorta* and *tibial artery*. Two other
323 significant tissues were from the digestive system; *esophagus muscularis* and *esophageal*
324 *mucosa*. We replicated these enrichment results in an independent dataset using a component
325 of the DEPICT⁶² tool that conducts a tissue-specific enrichment analysis on microarray-based
326 gene expression data (**Supplementary Methods**). DEPICT highlighted four tissues (**Figure 3**
327 **and Supplementary Table 20**) with significant enrichment of genes within the migraine loci;

328 arteries ($P = 1.58 \times 10^{-5}$), the upper gastrointestinal tract ($P = 2.97 \times 10^{-3}$), myometrium ($P =$
329 3.03×10^{-3}), and stomach ($P = 3.38 \times 10^{-3}$).

330

331 Taken together, the expression analyses implicate arterial and gastrointestinal (GI) tissues. To
332 discover if this enrichment signature could be attributed to a more specific type of smooth
333 muscle, we examined the expression of the nearest genes at migraine loci in a panel of 60
334 types of human smooth muscle tissue⁶³. Overall, migraine loci genes were not significantly
335 enriched in a particular class of smooth muscle (**Supplementary Figures 11-13**). This suggests
336 that the enrichment of migraine disease variants in genes expressed in tissues with a smooth
337 muscle component is not specific to blood vessels, the stomach or GI tract, but rather appears
338 to be generalizable across vascular and visceral smooth muscle types.

339

340 Combined, these results suggest that some of the genes affected by migraine-associated
341 variants are highly expressed in vascular tissues and their dysfunction could play a role in
342 migraine. Furthermore, the enrichment results suggest that other tissue types (e.g. smooth
343 muscle) could also play a role and this may become evident once more migraine loci are
344 discovered.

345

346 Enrichment in tissue-specific enhancers

347 To further assess the hypothesis that migraine variants might operate via effects on gene-
348 regulation, we investigated the degree of overlap with histone modifications. We identified
349 candidate causal variants underlying the 38 migraine loci, and examined their enrichment within
350 cell-type specific enhancers from 56 primary human tissues and cell types from the Roadmap
351 Epigenomics⁶⁴ and ENCODE projects⁶⁵ (**Online Methods** and **Supplementary Table 21**).
352 Candidate causal variants showed highest enrichment in tissues from the mid-frontal lobe and
353 duodenum smooth muscle, but these enrichments were not significant after adjusting for
354 multiple testing (**Figure 4**).

355

356 Gene set enrichment analyses

357 To implicate underlying biological pathways involved in migraine, we applied a Gene Ontology
358 (GO) over-representation analysis of the 38 migraine loci (**Online Methods**). We found nine
359 vascular-related biological function categories that are significantly enriched after correction for
360 multiple testing (**Supplementary Table 22**). Interestingly, we found little statistical support from
361 the identified loci for some molecular processes that have been previously linked to migraine,

362 e.g. ion homeostasis, glutamate signaling, serotonin signaling, nitric oxide signaling, and
363 oxidative stress (**Supplementary Table 23**). However, it is possible that the lack of enrichment
364 for these functions may be explained by recognizing that current annotations for many genes
365 and pathways are far from comprehensive, or that larger numbers of migraine loci need to be
366 identified before we have sensitivity to detect enrichment in these mechanisms.

367
368 For a more comprehensive pathway analysis we used DEPICT, which incorporates gene co-
369 expression information from microarray data to implicate additional, functionally less well-
370 characterized genes in known biological pathways, protein-protein complexes and mouse
371 phenotypes⁶² (by forming so-called ‘reconstituted gene sets’). From DEPICT we identified 67
372 reconstituted gene sets that are significantly enriched (FDR < 5%) for genes found among the
373 38 migraine associated loci (**Supplementary Table 24**). Because the reconstituted gene sets
374 had genes in common, we clustered them into 10 distinct groups of gene sets (**Figure 5 and**
375 **Online Methods**). Several gene sets, including the most significantly enriched reconstituted
376 gene set (*Abnormal Vascular Wound Healing*; $P = 1.86 \times 10^{-6}$), were grouped into clusters
377 related to cell-cell interactions (*ITGB1 PPI*, *Adherens Junction*, *Integrin Complex*). Several of
378 the other gene set clusters were also related to vascular-biology (**Figure 5 and Supplementary**
379 **Table 24**).

380

381 Discussion

382 In what is the largest genetic study of migraine to date, we identified 38 distinct genomic loci
383 harboring 44 independent susceptibility markers for the prevalent forms of migraine. We provide
384 evidence that migraine-associated genes are involved both in arterial and smooth muscle
385 function. Two separate analyses, the DEPICT and the GTEx gene-expression enrichment
386 analyses, point to vascular and smooth muscle tissues being involved in common variant
387 susceptibility to migraine. The vascular finding is consistent with known co-morbidities and
388 previously reported shared polygenic risk between migraine, stroke and cardiovascular
389 diseases^{66,67}. Furthermore, a recent GWA study of Cervical Artery Dissection (CeAD) identified
390 a genome-wide significant association at exactly the same index SNP (rs9349379) as is
391 associated to migraine in the *PHACTR1* locus, suggesting the possibility of partially shared
392 genetic components between migraine and CeAD²⁶. These results suggest that vascular
393 dysfunction and possibly also other smooth muscle dysfunction likely play roles in migraine
394 pathogenesis.

395

396 The support for vascular and smooth muscle enrichment of the loci is strong, with multiple lines
397 of evidence from independent methods and independent datasets. However, it remains likely
398 that neurogenic mechanisms are also involved in migraine. For example, several lines of
399 evidence from previous studies have pointed to such mechanisms^{5,68-71}. We found some
400 support for this when looking at gene expression of individual genes at the 38 loci
401 (**Supplementary Figure 2** and **Supplementary Table 25**), where many specific genes were
402 active in brain tissues. While we did not observe statistically significant enrichment in brain
403 across all loci, it may be that more associated loci are needed to detect this. Alternatively, it
404 could be due to difficulties in collecting appropriate brain tissue samples with enough specificity,
405 or other technical challenges. Additionally, there is less clarity of the biological mechanisms for
406 a brain disease like migraine compared to some other common diseases, e.g. autoimmune or
407 cardio-metabolic diseases where intermediate risk factors and underlying mechanisms are
408 better understood.

409
410 Interestingly, some of the analyses highlight gastrointestinal tissues. Although migraine attacks
411 may include gastrointestinal symptoms (e.g. nausea, vomiting, diarrhea)⁷² it is likely that the
412 signals observed here broadly represent smooth muscle signals rather than gastrointestinal
413 specificity. Smooth muscle is a predominant tissue of the intestine, yet specific smooth muscle
414 subtypes were not available to test this hypothesis in our primary enrichment analyses. We
415 showed instead in a range of 60 smooth muscle subtypes, that the migraine loci are expressed
416 in many types of smooth muscle, including vascular (**Supplementary Figure 12 and 13**). These
417 results, while not conclusive, suggest that the enrichment of the migraine loci in smooth muscle
418 is not specific to the stomach and GI tract.

419
420 Our results implicate cellular pathways and provide an opportunity to determine whether the
421 genomic data supports previously presented hypotheses of pathways linked to migraine. One
422 prevailing hypothesis stimulated by findings in familial hemiplegic migraine (FHM) has been that
423 migraine is a channelopathy^{5,21}. Among the 38 migraine loci only two harbor known ion channels
424 (*KCNK5*¹⁹ and *TRPM8*²⁰), while three additional loci (*SLC24A3*²², *ITPK1*²³, and *GJA1*²⁴) can be
425 linked to ion homeostasis. This further supports the findings of previous studies that in common
426 forms of migraine, ion channel dysfunction is not the major pathophysiological mechanism¹⁵.
427 However, more generally, genes involved in ion homeostasis could be a component of the
428 genetic susceptibility. Moreover, we cannot exclude that ion channels could still be important
429 contributors in migraine with aura, the form most closely resembling FHM, as our ability to

430 identify loci in this subgroup is more challenging. Another suggested hypothesis relates to
431 oxidative stress and nitric oxide (NO) signaling⁷³⁻⁷⁵. Six genes with known links to oxidative
432 stress and NO, within these 38 loci were identified (*REST*⁴⁴, *GJA1*⁴⁵, *YAP1*⁴⁶, *PRDM16*⁴⁷,
433 *LRP1*⁴⁸, and *MRVI1*⁴⁹). This is in line with previous findings¹¹, however, the DEPICT pathway
434 analysis observed no association between NO-related reconstituted gene sets and migraine
435 (*FDR* > 0.54, **Supplementary Table 23**).

436
437 Notably, in the migraine subtype analyses, it was possible to identify specific loci for migraine
438 without aura but not for migraine with aura. However, the heterogeneity analysis
439 (**Supplementary Tables 12-13**) demonstrated that most of the identified loci are implicated in
440 both migraine subtypes. This suggests that no loci were identified in the migraine with aura
441 analysis mainly due to lack of power from the reduced sample size. Additionally, as shown by
442 the LD score analysis (**Supplementary Figures 5-7**), the amount of heritability captured by the
443 migraine with aura dataset is considerably lower than migraine without aura, such that in order
444 to reach comparable power, a sample size of two- to three-times larger would be required. This
445 may reflect a higher degree of heterogeneity in the clinical capture, more complex underlying
446 biology, or even a larger contribution from low-frequency and rare variation to migraine risk for
447 this form of the disease.

448
449 In conclusion, the 38 genomic loci identified in this study support the notion that factors in
450 vascular and smooth muscle tissues contribute to migraine pathophysiology and that the two
451 major subtypes of migraine, migraine with aura and migraine without aura, have a partially
452 shared underlying genetic susceptibility profile.

453 URLs

454 1000 Genomes Project, <http://www.1000genomes.org/>; BEAGLE,
455 <http://faculty.washington.edu/browning/beagle/beagle.html>; DEPICT,
456 www.broadinstitute.org/mpg/depict; Fine-mapping loci with credible sets,
457 <https://github.com/hailianghuang/FM-summary>; GTEx, www.gtexportal.org; GWAMA,
458 <http://www.well.ox.ac.uk/gwama/>; IMPUTE2,
459 https://mathgen.stats.ox.ac.uk/impute/impute_v2.html; International Headache Genetics
460 Consortium, <http://www.headachegenetics.org/>; MACH,
461 <http://www.sph.umich.edu/csg/abecasis/MACH/tour/imputation.html>; matSpD,
462 <http://neurogenetics.qimrberghofer.edu.au/matSpD>; MINIMAC,
463 <http://genome.sph.umich.edu/wiki/Minimac>; PLINK, <http://pngu.mgh.harvard.edu/~purcell/plink/>;
464 ProbABEL, <http://www.genabel.org/packages/ProbABEL>; R, <https://www.r-project.org/>;
465 Roadmap Epigenomics Project, <http://www.roadmapepigenomics.org/>; SHAPEIT,
466 http://mathgen.stats.ox.ac.uk/genetics_software/shapeit/shapeit.v778.html; SNPTEST,
467 https://mathgen.stats.ox.ac.uk/genetics_software/snpTest/snpTest.html.
468

469 Acknowledgments

470 We would like to thank the numerous individuals who contributed to sample collection, storage,
471 handling, phenotyping and genotyping within each of the individual cohorts. We also thank the
472 important contribution to research made by the study participants. We are grateful to Huiying
473 Zhao (QIMR Berghofer Medical Research Institute) for helpful correspondence on the pathway
474 analyses. We acknowledge the support and contribution of pilot data from the GTEx consortium.
475 A list of study-specific acknowledgements can be found in the Supplementary Note.
476

477 Author Contributions

478 P.G., V.An., G.W.M., M.Ku., M.Kals., R.Mäg., K.P., E.H., E.L., A.G.U., L.C., E.M., L.M., A-L.E.,
479 A.F.C., T.F.H., A.J.A., D.I.C., and D.R.N. performed the experiments. P.G., V.An., B.S.W., P.P.,
480 T.E., T.H.P., K-H.F., M.Mu., N.A.F., A.I., G.McM., L.L., S.G.G., S.St., L.Q., H.H.H.A., D.A.H., J-
481 J.H., R.Mal., A.E.B., E.S., C.M.v.D., E.M., D.P.S., N.E., B.M.N., D.I.C., and D.R.N. performed
482 the statistical analyses. P.G., V.An., B.S.W., P.P., T.E., T.H.P., K-H.F., E.C-L., N.A.F., A.I.,
483 G.McM., L.L., M.Kall., T.M.F., S.G.G., S.St., M.Ko., L.Q., H.H.H.A., T.L., J.W., D.A.H., S.M.R.,

484 M.F., V.Ar., M.Kau., S.V., R.Mal., M.Ku., M.Kals., R.Mäg., K.P., H.H., A.E.B., J.H., E.S., C.S.,
485 C.W., Z.C., K.H., E.L., L.M.P, A-L.E., A.F.C., T.F.H., J.K., A.J.A., O.R., M.A.I., M-R.J., D.P.S.,
486 M.W., G.D.S., N.E., M.J.D., B.M.N., J.O., D.I.C., D.R.N., and A.P. participated in data
487 analysis/interpretation. P.G., V.An., B.S.W., T.H.P., K-H.F., E.C-L., T.K., G.M.T, M.Kall., C.R.,
488 A.H.S., G.B., M.Ko., T.L., M.S., M.G.H., M.F., V.Ar., M.Kau., S.V., R.Mal., A.C.H., P.A.F.M.,
489 N.G.M., G.W.M., H.H., A.E.B., L.F., J.H., P.H.L., C.S., C.W., Z.C., B.M-M., S.Sc., T.M., J.G.E.,
490 V.S., A.G.U., C.M.v.D., A.S., C.S.N., H.G., A-L.E., A.F.C., T.F.H., T.W., A.J.A., O.R., M-R.J.,
491 C.K., M.D.F., A.C.B., M.D., M.W., J-A.Z., B.M.N., J.O., D.I.C., D.R.N., and A.P. contributed
492 materials/analysis tools. T.E., T.K., T.L., H.S., B.W.J.H.P., A.C.H., P.A.F.M., N.G.M., G.W.M.,
493 L.F., A.H., A.S., C.S.N., M.Mä., T.W., J.K., O.R., M.A.I., T.S., M-R.J., A.M., C.K., D.P.S., M.D.F.,
494 A.M.J.M.v.d.M., J-A.Z., D.I.B., G.D.S., K.S., N.E., B.M.N., J.O., D.I.C., D.R.N., and A.P.
495 supervised the research. T.K., G.M.T, G.B., T.L., J.E.B., M.S., P.M.R., H.S., B.W.J.H.P., A.C.H.,
496 P.A.F.M., N.G.M., G.W.M., L.F., V.S., A.H., L.C., A.S., C.S.N., H.G., J.K., A.J.A., O.R., M.A.I.,
497 M-R.J., A.M., C.K., D.P.S., M.D., A.M.J.M.v.d.M., D.I.B., G.D.S., N.E., M.J.D., B.M.N., D.I.C.,
498 D.R.N., and A.P. conceived and designed the study. P.G., V.An., B.S.W., P.P., T.E., T.H.P.,
499 E.C-L., H.H., B.M.N., J.O., D.I.C., D.R.N., and A.P. wrote the paper. All authors contributed to
500 the final version of the manuscript.

501

502 Data access

503 All genome-wide significant and suggestive SNP associations ($P < 1 \times 10^{-5}$) from the meta-
504 analysis can be obtained directly from the IHGC website (<http://www.headachegenetics.org/>).
505 For access to deeper-level data please contact the data access committee ([fimm-](mailto:fimm-dac@helsinki.fi)
506 [dac@helsinki.fi](mailto:fimm-dac@helsinki.fi)).

507

508 References

- 509 1. Vos, T. *et al.* Years lived with disability (YLDs) for 1160 sequelae of 289 diseases and
510 injuries 1990-2010: A systematic analysis for the Global Burden of Disease Study 2010.
511 *Lancet* **380**, 2163–2196 (2012).
- 512 2. Vos, T. *et al.* Global, regional, and national incidence, prevalence, and years lived with
513 disability for 301 acute and chronic diseases and injuries in 188 countries, 1990–2013: a
514 systematic analysis for the Global Burden of Disease Study 2013. *Lancet* (2015).
515 doi:10.1016/S0140-6736(15)60692-4
- 516 3. Gustavsson, A. *et al.* Cost of disorders of the brain in Europe 2010. *Eur.*
517 *Neuropsychopharmacol.* **21**, 718–779 (2011).

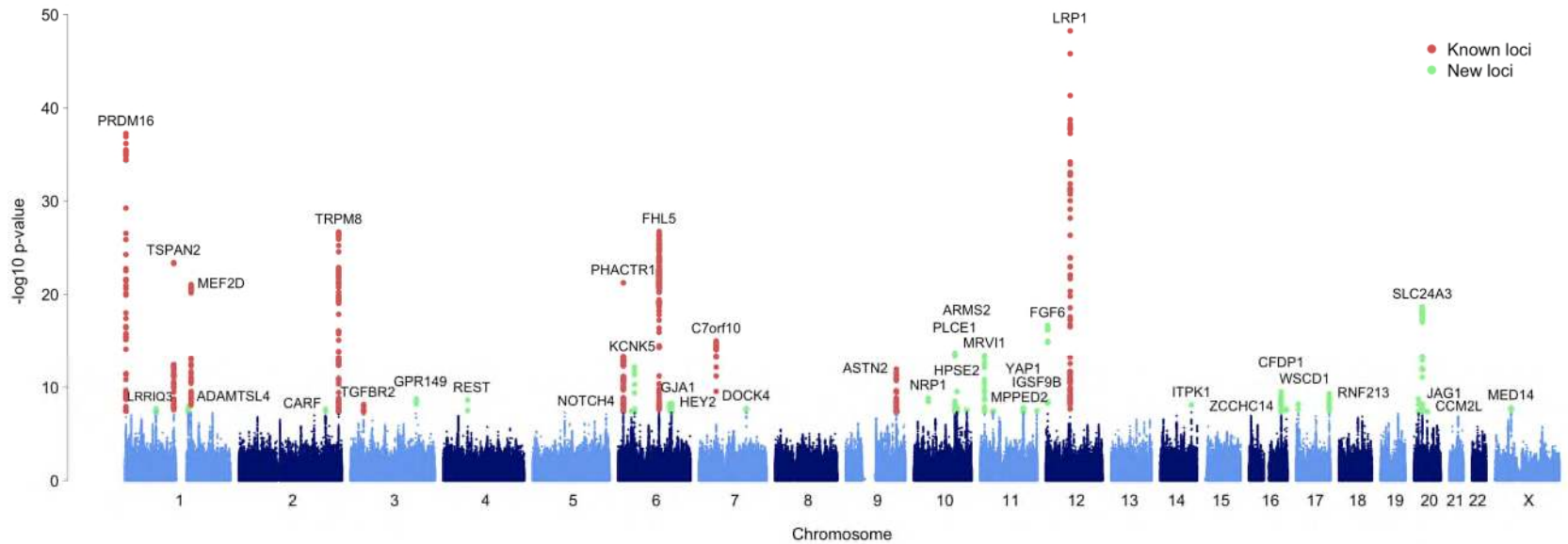
- 518 4. Pietrobon, D. & Striessnig, J. Neurological diseases: Neurobiology of migraine. *Nature*
519 *Reviews Neuroscience* **4**, 386–398 (2003).
- 520 5. Tfelt-Hansen, P. C. & Koehler, P. J. One hundred years of migraine research: Major
521 clinical and scientific observations from 1910 to 2010. *Headache* **51**, 752–778 (2011).
- 522 6. Society, H. C. C. of the I. H. The International Classification of Headache Disorders: 2nd
523 edition. *Cephalalgia* **24**, 1–160 (2004).
- 524 7. Polderman, T. J. C. *et al.* Meta-analysis of the heritability of human traits based on fifty
525 years of twin studies. *Nat. Genet.* **47**, 702–709 (2015).
- 526 8. Anttila, V. *et al.* Genome-wide association study of migraine implicates a common
527 susceptibility variant on 8q22.1. *Nat. Genet.* **42**, 869–873 (2010).
- 528 9. Chasman, D. I. *et al.* Genome-wide association study reveals three susceptibility loci for
529 common migraine in the general population. *Nat Genet* **43**, 695–698 (2011).
- 530 10. Freilinger, T. *et al.* Genome-wide association analysis identifies susceptibility loci for
531 migraine without aura. *Nat. Genet.* **44**, 777–782 (2012).
- 532 11. Anttila, V. *et al.* Genome-wide meta-analysis identifies new susceptibility loci for migraine.
533 *Nat. Genet.* **45**, 912–7 (2013).
- 534 12. Ophoff, R. A. *et al.* Familial hemiplegic migraine and episodic ataxia type-2 are caused by
535 mutations in the Ca²⁺ channel gene CACNL1A4. *Cell* **87**, 543–552 (1996).
- 536 13. De Fusco, M. *et al.* Haploinsufficiency of ATP1A2 encoding the Na⁺/K⁺ pump alpha2
537 subunit associated with familial hemiplegic migraine type 2. *Nat. Genet.* **33**, 192–196
538 (2003).
- 539 14. Dichgans, M. *et al.* Mutation in the neuronal voltage-gated sodium channel SCN1A in
540 familial hemiplegic migraine. *Lancet* **366**, 371–377 (2005).
- 541 15. Nyholt, D. R. *et al.* A high-density association screen of 155 ion transport genes for
542 involvement with common migraine. *Hum. Mol. Genet.* **17**, 3318–3331 (2008).
- 543 16. Altshuler, D. M. *et al.* An integrated map of genetic variation from 1,092 human genomes.
544 *Nature* **491**, 56–65 (2012).
- 545 17. Chasman, D. I. *et al.* Selectivity in Genetic Association with Sub-classified Migraine in
546 Women. *PLoS Genet.* **10**, (2014).
- 547 18. Han, B. & Eskin, E. Random-effects model aimed at discovering associations in meta-
548 analysis of genome-wide association studies. *Am. J. Hum. Genet.* **88**, 586–598 (2011).
- 549 19. Morton, M. J., Abohamed, A., Sivaprasadarao, A. & Hunter, M. pH sensing in the two-
550 pore domain K⁺ channel, TASK2. *Proc. Natl. Acad. Sci. U. S. A.* **102**, 16102–16106
551 (2005).

- 552 20. Ramachandran, R. *et al.* TRPM8 activation attenuates inflammatory responses in mouse
553 models of colitis. *Proc. Natl. Acad. Sci. U. S. A.* **110**, 7476–81 (2013).
- 554 21. Hanna, M. G. Genetic neurological channelopathies. *Nat. Clin. Pract. Neurol.* **2**, 252–263
555 (2006).
- 556 22. Kraev, A. *et al.* Molecular cloning of a third member of the potassium-dependent sodium-
557 calcium exchanger gene family, NCKX3. *J. Biol. Chem.* **276**, 23161–72 (2001).
- 558 23. Ismailov, I. I. *et al.* A biologic function for an ‘orphan’ messenger: D-myo-inositol 3,4,5,6-
559 tetrakisphosphate selectively blocks epithelial calcium-activated chloride channels. *Proc.*
560 *Natl. Acad. Sci. U. S. A.* **93**, 10505–9 (1996).
- 561 24. De Bock, M. *et al.* Connexin channels provide a target to manipulate brain endothelial
562 calcium dynamics and blood-brain barrier permeability. *J. Cereb. Blood Flow Metab.* **31**,
563 1942–1957 (2011).
- 564 25. Kathiresan, S. *et al.* Genome-wide association of early-onset myocardial infarction with
565 single nucleotide polymorphisms and copy number variants. *Nat. Genet.* **41**, 334–341
566 (2009).
- 567 26. Debette, S. *et al.* Common variation in PHACTR1 is associated with susceptibility to
568 cervical artery dissection. *Nat. Genet.* **47**, 78–83 (2015).
- 569 27. Law, C. *et al.* Clinical features in a family with an R460H mutation in transforming growth
570 factor beta receptor 2 gene. *J Med Genet* **43**, 908–916 (2006).
- 571 28. Bown, M. J. *et al.* Abdominal aortic aneurysm is associated with a variant in low-density
572 lipoprotein receptor-related protein 1. *Am. J. Hum. Genet.* **89**, 619–627 (2011).
- 573 29. Arndt, A. K. *et al.* Fine mapping of the 1p36 deletion syndrome identifies mutation of
574 PRDM16 as a cause of cardiomyopathy. *Am. J. Hum. Genet.* **93**, 67–77 (2013).
- 575 30. Fujimura, M. *et al.* Genetics and Biomarkers of Moyamoya Disease: Significance of
576 RNF213 as a Susceptibility Gene. *J. stroke* **16**, 65–72 (2014).
- 577 31. McElhinney, D. B. *et al.* Analysis of cardiovascular phenotype and genotype-phenotype
578 correlation in individuals with a JAG1 mutation and/or Alagille syndrome. *Circulation* **106**,
579 2567–2574 (2002).
- 580 32. Bezzina, C. R. *et al.* Common variants at SCN5A-SCN10A and HEY2 are associated with
581 Brugada syndrome, a rare disease with high risk of sudden cardiac death. *Nat. Genet.*
582 **45**, 1044–9 (2013).
- 583 33. Sinner, M. F. *et al.* Integrating genetic, transcriptional, and functional analyses to identify
584 five novel genes for atrial fibrillation. *Circulation* (2014).
585 doi:10.1161/CIRCULATIONAHA.114.009892

- 586 34. Neale, B. M. *et al.* Genome-wide association study of advanced age-related macular
587 degeneration identifies a role of the hepatic lipase gene (LIPC). *Proc. Natl. Acad. Sci. U.*
588 *S. A.* **107**, 7395–7400 (2010).
- 589 35. Desch, M. *et al.* IRAG determines nitric oxide- and atrial natriuretic peptide-mediated
590 smooth muscle relaxation. *Cardiovasc. Res.* **86**, 496–505 (2010).
- 591 36. Lang, N. N., Luksha, L., Newby, D. E. & Kublickiene, K. Connexin 43 mediates
592 endothelium-derived hyperpolarizing factor-induced vasodilatation in subcutaneous
593 resistance arteries from healthy pregnant women. *Am. J. Physiol. Heart Circ. Physiol.*
594 **292**, H1026–H1032 (2007).
- 595 37. Dong, H., Jiang, Y., Triggle, C. R., Li, X. & Lytton, J. Novel role for K⁺-dependent
596 Na⁺/Ca²⁺ exchangers in regulation of cytoplasmic free Ca²⁺ and contractility in arterial
597 smooth muscle. *Am. J. Physiol. Heart Circ. Physiol.* **291**, H1226–H1235 (2006).
- 598 38. Yamaji, M., Mahmoud, M., Evans, I. M. & Zachary, I. C. Neuropilin 1 is essential for
599 gastrointestinal smooth muscle contractility and motility in aged mice. *PLoS One* **10**,
600 e0115563 (2015).
- 601 39. Lu, X. *et al.* Genome-wide association study in Han Chinese identifies four new
602 susceptibility loci for coronary artery disease. *Nature Genetics* **44**, 890–894 (2012).
- 603 40. Hager, J. *et al.* Genome-wide association study in a Lebanese cohort confirms PHACTR1
604 as a major determinant of coronary artery stenosis. *PLoS One* **7**, (2012).
- 605 41. Coronary, T., Disease, A. & Consortium, G. A genome-wide association study in
606 Europeans and South Asians identifies five new loci for coronary artery disease. *Nat.*
607 *Genet.* **43**, 339–44 (2011).
- 608 42. Odonnell, C. J. *et al.* Genome-wide association study for coronary artery calcification with
609 follow-up in myocardial infarction. *Circulation* **124**, 2855–2864 (2011).
- 610 43. Porcu, E. *et al.* A meta-analysis of thyroid-related traits reveals novel loci and gender-
611 specific differences in the regulation of thyroid function. *PLoS Genet.* **9**, e1003266 (2013).
- 612 44. Lu, T. *et al.* REST and stress resistance in ageing and Alzheimer disease. *Nature Epub*
613 **ahead**, 448–54 (2014).
- 614 45. Kar, R., Riquelme, M. A., Werner, S. & Jiang, J. X. Connexin 43 channels protect
615 osteocytes against oxidative stress-induced cell death. *J. Bone Miner. Res.* **28**, 1611–
616 1621 (2013).
- 617 46. Dixit, D., Ghildiyal, R., Anto, N. P. & Sen, E. Chaetocin-induced ROS-mediated apoptosis
618 involves ATM-YAP1 axis and JNK-dependent inhibition of glucose metabolism. *Cell*
619 *Death Dis.* **5**, e1212 (2014).

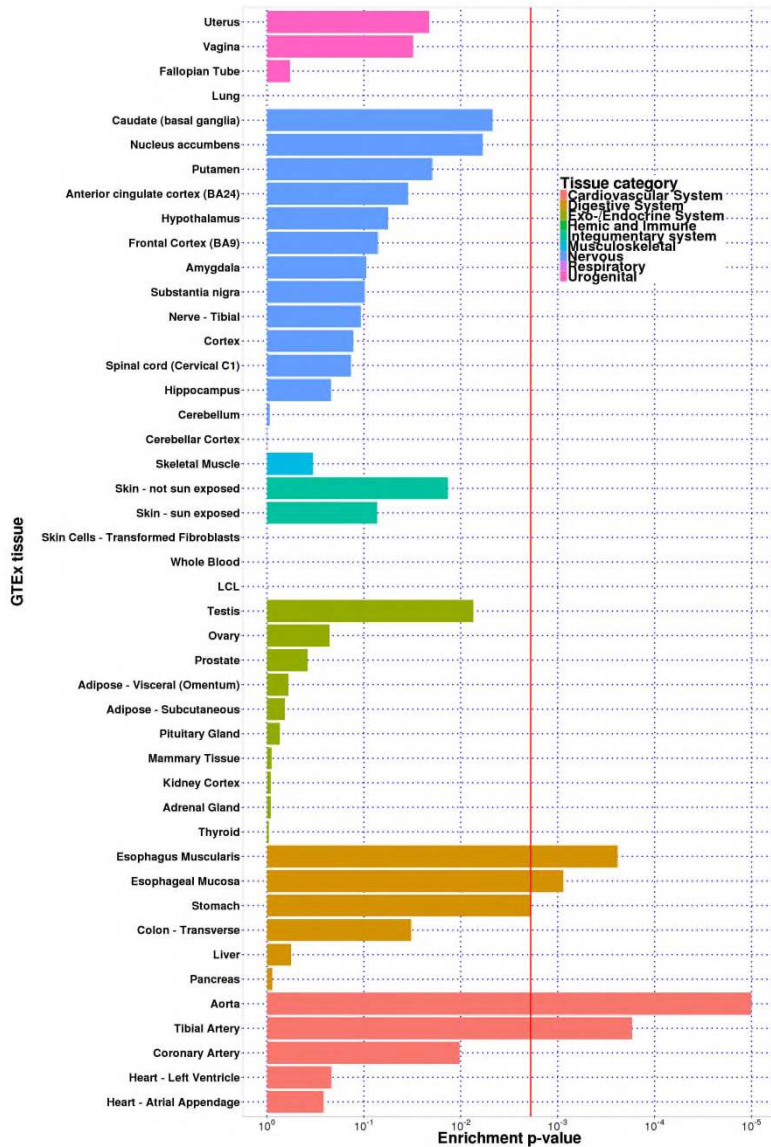
- 620 47. Chuikov, S., Levi, B. P., Smith, M. L. & Morrison, S. J. Prdm16 promotes stem cell
621 maintenance in multiple tissues, partly by regulating oxidative stress. *Nat. Cell Biol.* **12**,
622 999–1006 (2010).
- 623 48. Castellano, J. *et al.* Hypoxia stimulates low-density lipoprotein receptor-related protein-1
624 expression through hypoxia-inducible factor-1 α in human vascular smooth muscle cells.
625 *Arterioscler. Thromb. Vasc. Biol.* **31**, 1411–1420 (2011).
- 626 49. Schlossmann, J. *et al.* Regulation of intracellular calcium by a signalling complex of
627 IRAG, IP3 receptor and cGMP kinase I β . *Nature* **404**, 197–201 (2000).
- 628 50. Nalls, M. a *et al.* Large-scale meta-analysis of genome-wide association data identifies
629 six new risk loci for Parkinson’s disease. *Nat. Genet.* **056**, 1–7 (2014).
- 630 51. Lambert, J. C. *et al.* Meta-analysis of 74,046 individuals identifies 11 new susceptibility
631 loci for Alzheimer’s disease. *Nat. Genet.* **45**, 1452–8 (2013).
- 632 52. Ripke, S. *et al.* Biological insights from 108 schizophrenia-associated genetic loci. *Nature*
633 **511**, 421–427 (2014).
- 634 53. Wood, A. R. *et al.* Defining the role of common variation in the genomic and biological
635 architecture of adult human height. *Nat. Genet.* **46**, 1173–86 (2014).
- 636 54. Purcell, S. *et al.* PLINK: a tool set for whole-genome association and population-based
637 linkage analyses. *Am. J. Hum. Genet.* **81**, 559–575 (2007).
- 638 55. Bulik-Sullivan, B. K. *et al.* LD Score regression distinguishes confounding from
639 polygenicity in genome-wide association studies. *Nat. Genet.* **47**, 291–295 (2015).
- 640 56. Yang, J. *et al.* Genomic inflation factors under polygenic inheritance. *Eur. J. Hum. Genet.*
641 **19**, 807–812 (2011).
- 642 57. Magi, R., Lindgren, C. M. & Morris, A. P. Meta-analysis of sex-specific genome-wide
643 association studies. *Genet. Epidemiol.* **34**, 846–853 (2010).
- 644 58. Maller, J. B. *et al.* Bayesian refinement of association signals for 14 loci in 3 common
645 diseases. *Nat. Genet.* **44**, 1294–301 (2012).
- 646 59. Nicolae, D. L. *et al.* Trait-associated SNPs are more likely to be eQTLs: Annotation to
647 enhance discovery from GWAS. *PLoS Genet.* **6**, (2010).
- 648 60. Maurano, M. T. *et al.* Systematic Localization of Common Disease-Associated Variation
649 in Regulatory DNA. *Science* **337**, 1190–1195 (2012).
- 650 61. Consortium, T. G. The Genotype-Tissue Expression (GTEx) project. *Nat. Genet.* **45**, 580–
651 5 (2013).
- 652 62. Pers, T. H. *et al.* Biological interpretation of genome-wide association studies using
653 predicted gene functions. *Nat. Commun.* **6**, 5890 (2015).

- 654 63. Chi, J. T. *et al.* Gene expression programs of human smooth muscle cells: Tissue-
655 specific differentiation and prognostic significance in breast cancers. *PLoS Genet.* **3**,
656 1770–1784 (2007).
- 657 64. Bernstein, B. E. *et al.* The NIH Roadmap Epigenomics Mapping Consortium. *Nat.*
658 *Biotechnol.* **28**, 1045–1048 (2010).
- 659 65. The ENCODE Project Consortium. An integrated encyclopedia of DNA elements in the
660 human genome. *Nature* **489**, 57–74 (2012).
- 661 66. Winsvold, B. S. *et al.* Genetic analysis for a shared biological basis between migraine and
662 coronary artery disease. *Neurol. Genet.* **1**, e10–e10 (2015).
- 663 67. Malik, R. *et al.* Shared genetic basis for migraine and ischemic stroke: A genome-wide
664 analysis of common variants. *Neurology* **84**, 2132–45 (2015).
- 665 68. Ferrari, M. D., Klever, R. R., Terwindt, G. M., Ayata, C. & van den Maagdenberg, A. M. J.
666 M. Migraine pathophysiology: lessons from mouse models and human genetics. *Lancet.*
667 *Neurol.* **14**, 65–80 (2015).
- 668 69. Olesen, J., Burstein, R., Ashina, M. & Tfelt-Hansen, P. Origin of pain in migraine:
669 evidence for peripheral sensitisation. *Lancet Neurol.* **8**, 679–690 (2009).
- 670 70. Hadjikhani, N. *et al.* Mechanisms of migraine aura revealed by functional MRI in human
671 visual cortex. *Proc. Natl. Acad. Sci.* **98**, 4687–4692 (2001).
- 672 71. Lauritzen, M. Pathophysiology of the migraine aura. The spreading depression theory.
673 *Brain* **117** (Pt 1, 199–210 (1994).
- 674 72. Headache Classification Committee of the International Headache Society (IHS). The
675 International Classification of Headache Disorders, 3rd edition (beta version). *Cephalalgia*
676 **33**, 629–808 (2013).
- 677 73. Olesen, J. The role of nitric oxide (NO) in migraine, tension-type headache and cluster
678 headache. *Pharmacol Ther* **120**, 157–171 (2008).
- 679 74. Ashina, M., Hansen, J. M. & Olesen, J. Pearls and pitfalls in human pharmacological
680 models of migraine: 30 years' experience. *Cephalalgia* **33**, 540–53 (2013).
- 681 75. Read, S. J. & Parsons, A. A. Sumatriptan modifies cortical free radical release during
682 cortical spreading depression: A novel antimigraine action for sumatriptan? *Brain Res.*
683 **870**, 44–53 (2000).
- 684



685
 686 **Figure 1.** Manhattan plot of the primary meta-analysis of all migraine (59,674 cases vs. 316,078 controls). Each marker was tested
 687 for association using an additive genetic model by logistic regression adjusted for sex. A fixed-effects meta-analysis was then used to
 688 combine the association statistics from all 22 clinic and population-based studies from the IHGC. The horizontal axis shows the
 689 chromosomal position and the vertical axis shows the significance of tested markers from logistic regression. Markers with test
 690 statistics that reach genome-wide significance ($P < 5 \times 10^{-8}$) at previously known and newly identified loci are highlighted according
 691 to the color legend.

692
 693
 694
 695
 696
 697



698

699 **Figure 2.** Gene expression enrichment of genes from the 38 migraine loci in GTEx tissues.

700 Expression data from 1,641 samples was obtained using RNAseq for 42 tissues and three cell

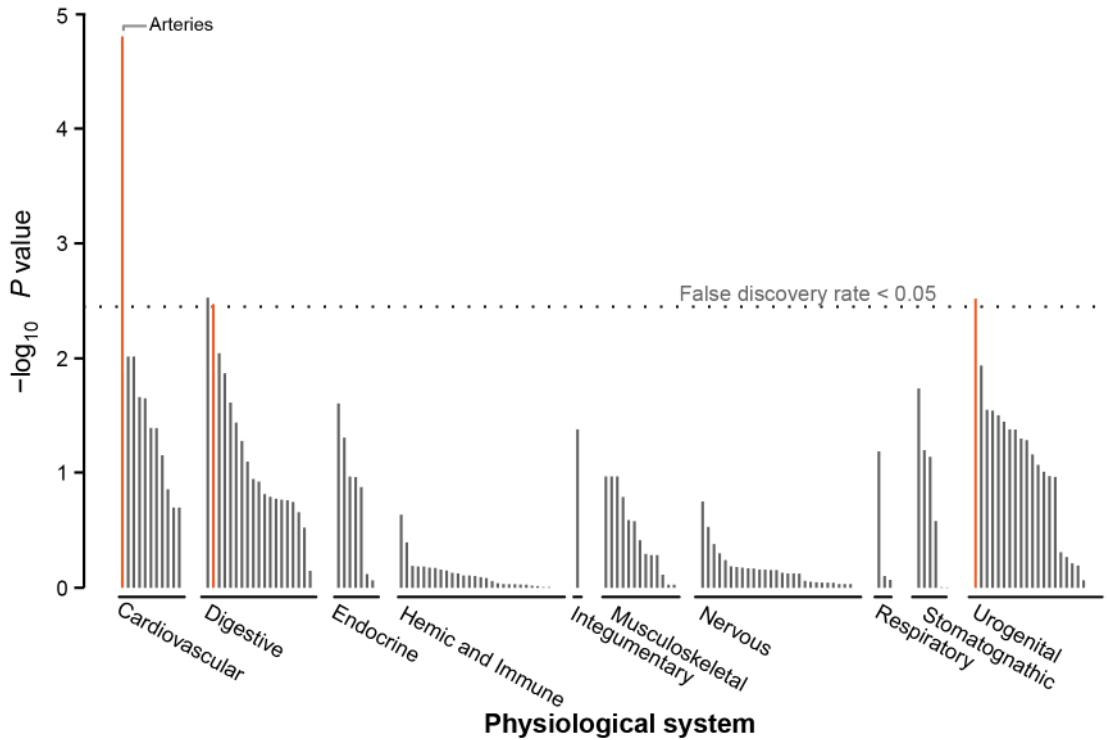
701 lines from the GTEx consortium. Enrichment *P*-values were assessed empirically for each tissue

702 using a permutation procedure (100,000 replicates) and the red vertical line shows the

703 significance threshold after adjusting for multiple testing by Bonferroni correction (see **Online**

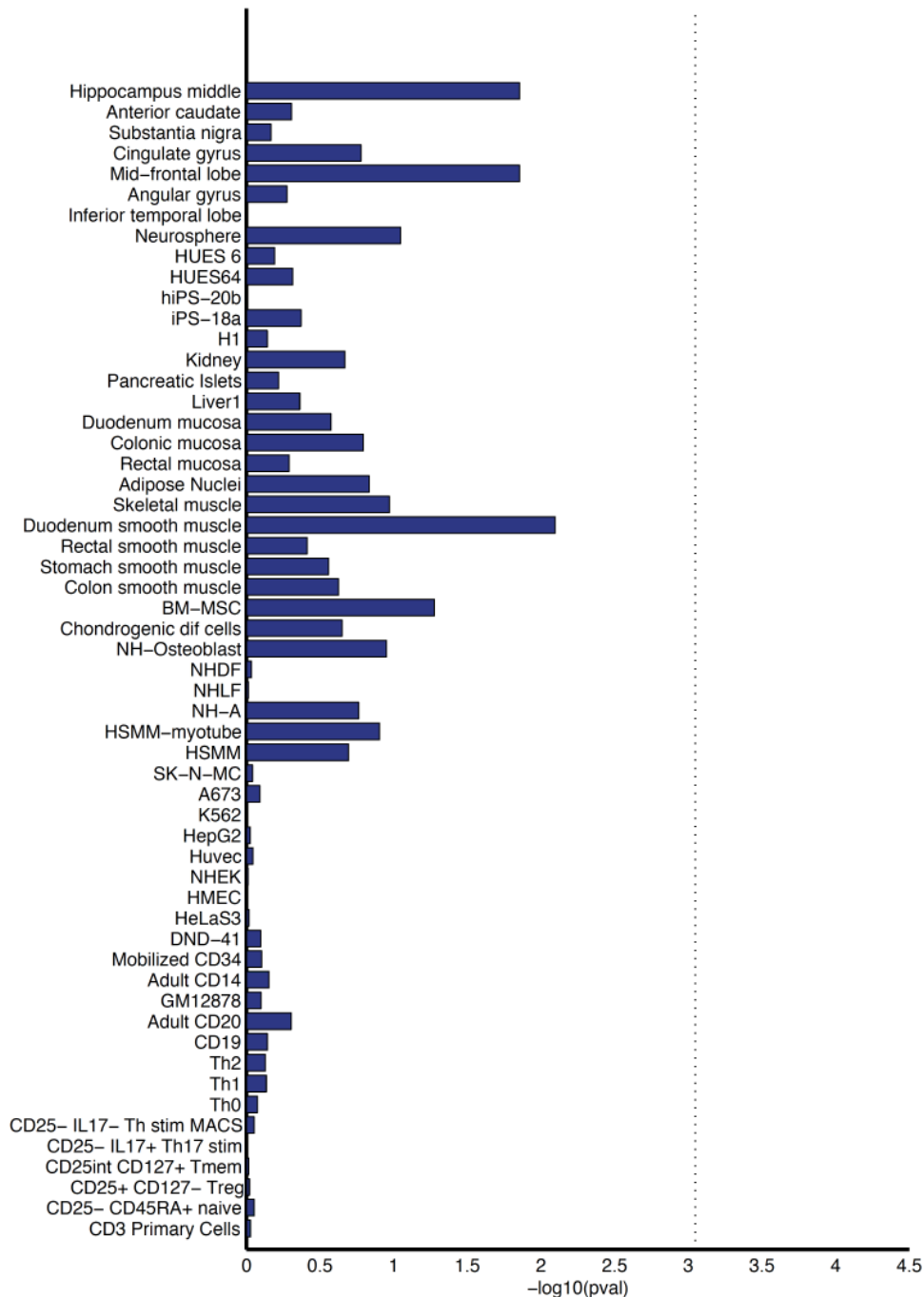
704 **Methods**).

705



706
707

708 **Figure 3.** Gene expression enrichment of genes from the 38 migraine loci in 209 tissue/cell type
 709 annotations by DEPICT. Expression data was obtained from 37,427 human microarray samples
 710 and then genes in the migraine loci were assessed for high expression in each of the annotation
 711 categories. Enrichment P -values were determined by comparing the expression pattern from the
 712 migraine loci to 500 randomly generated loci and the false discovery rate (horizontal dashed
 713 line) was estimated to control for multiple testing (see **Online Methods**). A full list of these
 714 enrichment results are provided in **Supplementary Table 20**.



715

716

717

718

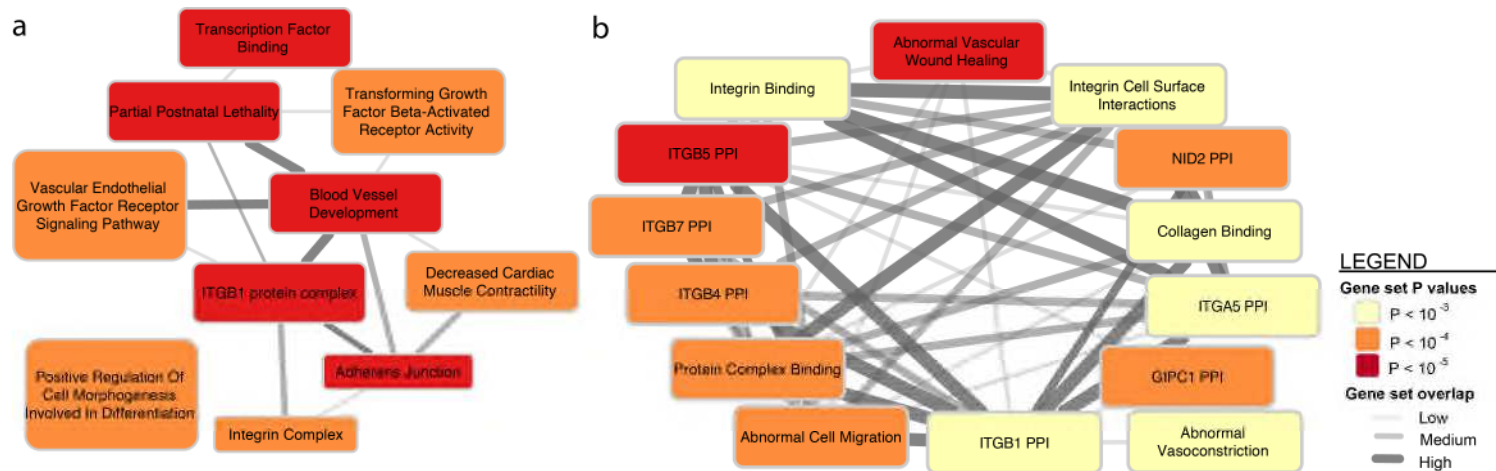
719

720

721

722

Figure 4. Enrichment of the migraine loci in sets of tissue-specific enhancers. We mapped credible sets from the migraine loci to sets of enhancers under active expression in 56 tissues and cell lines (identified by H3K27ac histone marks from the Roadmap Epigenomics⁶⁴ and ENCODE⁶⁵ projects). Enrichment *P*-values were assessed empirically by randomly generating a background set of matched loci for comparison (10,000 replicates) and the vertical dotted line is the significance threshold after adjusting for 56 separate tests by Bonferroni correction (see **Online Methods**).



723

724 **Figure 5.** DEPICT network of the reconstituted gene sets that were found to be significantly enriched (false discovery rate < 0.05) for
 725 genes at the migraine loci (**Online Methods**). Enriched gene sets are represented as nodes with pairwise overlap denoted by the
 726 width of the connecting lines and empirical enrichment *P*-value is indicated by color intensity (darker is more significant). The 67
 727 significantly enriched gene sets were then clustered by similarity into 10 group nodes as shown in **(a)** where each group node is
 728 named after the most representative gene set in the group. **(b)** Shows one example of the enriched reconstituted gene sets that were
 729 clustered within the now expanded *ITGB1 PPI* group. A full list of the 67 significantly enriched reconstituted gene sets can be found
 730 in **Supplementary Table 24**.

731 **Table 1.** Individual IHGC GWA studies listed with cases and control numbers used in the primary analysis (all migraine) and in the
732 subtype analyses (migraine with aura and migraine without aura). Note that chromosome X genotype data was unavailable from
733 three of the individual GWA studies (EGCUT, Rotterdam III, and TwinsUK) and also partially unavailable from some of the control
734 samples (specifically the GSK controls) used for the ‘German MO’ study, meaning that the number of samples analyzed on
735 chromosome X was 57,756 cases and 299,109 controls. Complete data was available on the autosomes for all samples.

736

GWA Study ID	Full Name of GWA Study	<u>All migraine</u>		<u>Migraine with aura</u>		<u>Migraine without aura</u>	
		Cases	Controls	Cases	Controls	Cases	Controls
23andMe	23andMe Inc.	30,465	143,147	-	-	-	-
ALSPAC	Avon Longitudinal Study of Parents and Children	3,134	5,103	-	-	-	-
ATM	Australian Twin Migraine	1,683	2,383	-	-	-	-
B58C	1958 British Birth Cohort	1,165	4,141	-	-	-	-
Danish HC	Danish Headache Center	1,771	1,000	775	1,000	996	1,000
DeCODE	deCODE Genetics Inc.	3,135	95,585	366	95,585	608	95,585
Dutch MA	Dutch migraine with aura	734	5,211	734	5,211	-	-
Dutch MO	Dutch migraine without aura	1,115	2,028	-	-	1,115	2,028
EGCUT	Estonian Genome Center, University of Tartu	813	9,850	76	9,850	94	9,850
Finnish MA	Finnish migraine with aura	933	2,715	933	2,715	-	-
German MA	German migraine with aura	1,071	1,010	1,071	1,010	-	-
German MO	German migraine without aura	1,160	1,647	-	-	1,160	1,647

Health 2000	Health 2000	136	1,764	-	-	-	-
HUNT	Nord-Trøndelag Health Study	1,395	1,011	290	1,011	980	1,011
NFBC	Northern Finnish Birth Cohort	756	4,393	-	-	-	-
NTR/NESDA	Netherlands Twin Register and the Netherlands Study of Depression and Anxiety	1,636	3,819	544	3,819	615	3,819
Rotterdam III	Rotterdam Study III	487	2,175	106	2,175	381	2,175
Swedish Twins	Swedish Twin Registry	1,307	4,182	-	-	-	-
Tromsø	The Tromsø Study	660	2,407	-	-	-	-
Twins UK	Twins UK	618	2,334	202	2,334	416	2,334
WGHS	Women's Genome Health Study	5,122	18,108	1,177	18,108	1,826	18,108
Young Finns	Young Finns	378	2,065	58	2,065	157	2,065
	Total:	59,674	316,078	6,332	144,883	8,348	139,622

737

738 **Table 2.** Summary of the 38 genomic loci associated with the prevalent types of migraine. Ten loci were previously reported
739 (PubMed IDs listed) and 28 are newly found in this study. For each locus, the nearest coding gene to the index SNP is given. Effect
740 sizes and *P*-values for each SNP were calculated for each study with an additive genetic model using logistic regression adjusted for
741 sex and then combined in a fixed-effects meta-analysis. For loci that contain a secondary LD-independent signal passing genome-
742 wide significance, the secondary index SNP and *P*-value is given. For the seven loci reaching genome-wide significance in the
743 migraine without aura sub-type analysis, the corresponding index SNP and *P*-value are also given. Evidence for significant
744 heterogeneity was found at four loci (*TRPM8*, *MRVI1*, *ZCCHC14*, and *CCM2L*) so for those we present the results of a random-
745 effects model.
746

Locus Rank	Nearest coding gene	Chr	Index SNP	Minor Allele	MAF	All Migraine		Secondary signal		Migraine without aura		Previous Publication PMID
						OR [95% CI]	P	Index SNP	P	Index SNP	P	
1	<i>LRP1</i>	12	rs11172113	C	0.42	0.90 [0.89-0.91]	5.6 x 10 ⁻⁴⁹	rs7961602	2.1 x 10 ⁻¹¹	rs11172113	4.3 x 10 ⁻¹⁶	21666692
2	<i>PRDM16</i>	1	rs10218452	G	0.22	1.11 [1.10-1.13]	5.3 x 10 ⁻³⁸	rs12135062	3.7 x 10 ⁻¹⁰	-	-	21666692
3	<i>FHL5</i>	6	rs67338227	T	0.23	1.09 [1.08-1.11]	2.0 x 10 ⁻²⁷	rs2223239	3.2 x 10 ⁻¹⁰	rs7775721	1.1 x 10 ⁻¹²	23793025
4	<i>TSPAN2</i>	1	rs2078371	C	0.12	1.11 [1.09-1.13]	4.1 x 10 ⁻²⁴	rs7544256	8.7 x 10 ⁻⁰⁹	rs2078371	7.4 x 10 ⁻⁰⁹	23793025
5	<i>TRPM8</i>	2	rs10166942	C	0.20	0.94 [0.89-0.99]	1.0 x 10 ⁻²³	rs566529	2.5 x 10 ⁻⁰⁹	rs6724624	1.1 x 10 ⁻⁰⁹	21666692
6	<i>PHACTR1</i>	6	rs9349379	G	0.41	0.93 [0.92-0.95]	5.8 x 10 ⁻²²	-	-	rs9349379	2.1 x 10 ⁻⁰⁹	22683712
7	<i>MEF2D</i>	1	rs1925950	G	0.35	1.07 [1.06-1.09]	9.1 x 10 ⁻²²	-	-	-	-	22683712
8	<i>SLC24A3</i>	20	rs4814864	C	0.26	1.07 [1.06-1.09]	2.2 x 10 ⁻¹⁹	-	-	-	-	-
9	<i>FGF6</i>	12	rs1024905	G	0.47	1.06 [1.04-1.08]	2.1 x 10 ⁻¹⁷	-	-	rs1024905	2.5 x 10 ⁻⁰⁹	-
10	<i>C7orf10</i>	7	rs186166891	T	0.11	1.09 [1.07-1.12]	9.7 x 10 ⁻¹⁶	-	-	-	-	23793025
11	<i>PLCE1</i>	10	rs10786156	G	0.45	0.95 [0.94-0.96]	2.0 x 10 ⁻¹⁴	rs75473620	5.8 x 10 ⁻⁰⁹	-	-	-
12	<i>KCNK5</i>	6	rs10456100	T	0.28	1.06 [1.04-1.07]	6.9 x 10 ⁻¹³	-	-	-	-	-
13	<i>ASTN2</i>	9	rs6478241	A	0.36	1.05 [1.04-1.07]	1.2 x 10 ⁻¹²	-	-	rs6478241	1.2 x 10 ⁻¹⁰	22683712
14	<i>MRVI1</i>	11	rs4910165	C	0.33	0.94 [0.91-0.98]	2.9 x 10 ⁻¹¹	-	-	-	-	-
15	<i>HPSE2</i>	10	rs12260159	A	0.07	0.92 [0.89-0.94]	3.2 x 10 ⁻¹⁰	-	-	-	-	-
16	<i>CFDP1</i>	16	rs77505915	T	0.45	1.05 [1.03-1.06]	3.3 x 10 ⁻¹⁰	-	-	-	-	-
17	<i>RNF213</i>	17	rs17857135	C	0.17	1.06 [1.04-1.08]	5.2 x 10 ⁻¹⁰	-	-	-	-	-
18	<i>NRP1</i>	10	rs2506142	G	0.17	1.06 [1.04-1.07]	1.5 x 10 ⁻⁰⁹	-	-	-	-	-

19	<i>GPR149</i>	3	rs13078967	C	0.03	0.87 [0.83-0.91]	1.8 x 10 ⁻⁰⁹	-	-	-	-	-
20	<i>JAG1</i>	20	rs111404218	G	0.34	1.05 [1.03-1.07]	2.0 x 10 ⁻⁰⁹	-	-	-	-	-
21	<i>REST</i>	4	rs7684253	C	0.45	0.96 [0.94-0.97]	2.5 x 10 ⁻⁰⁹	-	-	-	-	-
22	<i>ZCCHC14</i>	16	rs4081947	G	0.34	1.03 [1.00-1.06]	2.5 x 10 ⁻⁰⁹	-	-	-	-	-
23	<i>HEY2</i>	6	rs1268083	C	0.48	0.96 [0.95-0.97]	5.3 x 10 ⁻⁰⁹	-	-	-	-	-
24	<i>WSCD1</i>	17	rs75213074	T	0.03	0.89 [0.86-0.93]	7.1 x 10 ⁻⁰⁹	-	-	-	-	-
25	<i>GJA1</i>	6	rs28455731	T	0.16	1.06 [1.04-1.08]	7.3 x 10 ⁻⁰⁹	-	-	-	-	-
26	<i>TGFBR2</i>	3	rs6791480	T	0.31	1.04 [1.03-1.06]	7.8 x 10 ⁻⁰⁹	-	-	-	-	22683712
27	<i>ITPK1</i>	14	rs11624776	C	0.31	0.96 [0.94-0.97]	7.9 x 10 ⁻⁰⁹	-	-	-	-	-
28	<i>ADAMTSL4</i>	1	rs6693567	C	0.27	1.05 [1.03-1.06]	1.2 x 10 ⁻⁰⁸	-	-	-	-	-
29	<i>CCM2L</i>	20	rs144017103	T	0.02	0.85 [0.76-0.96]	1.2 x 10 ⁻⁰⁸	-	-	-	-	-
30	<i>YAP1</i>	11	rs10895275	A	0.33	1.04 [1.03-1.06]	1.6 x 10 ⁻⁰⁸	-	-	-	-	-
31	<i>MED14</i>	X	rs12845494	G	0.27	0.96 [0.95-0.97]	1.7 x 10 ⁻⁰⁸	-	-	-	-	-
32	<i>DOCK4</i>	7	rs10155855	T	0.05	1.08 [1.05-1.12]	2.1 x 10 ⁻⁰⁸	-	-	-	-	-
33	<i>LRR1Q3</i>	1	rs1572668	G	0.48	1.04 [1.02-1.05]	2.1 x 10 ⁻⁰⁸	-	-	-	-	-
34	<i>CARF</i>	2	rs138556413	T	0.03	0.88 [0.84-0.92]	2.3 x 10 ⁻⁰⁸	-	-	-	-	-
35	<i>ARMS2</i>	10	rs2223089	C	0.08	0.93 [0.91-0.95]	3.0 x 10 ⁻⁰⁸	-	-	-	-	-
36	<i>IGSF9B</i>	11	rs561561	T	0.12	0.94 [0.92-0.96]	3.4 x 10 ⁻⁰⁸	-	-	-	-	-
37	<i>MPPED2</i>	11	rs11031122	C	0.24	1.04 [1.03-1.06]	3.5 x 10 ⁻⁰⁸	-	-	-	-	-
38	<i>NOTCH4</i>	6	rs140002913	A	0.06	0.91 [0.88-0.94]	3.8 x 10 ⁻⁰⁸	-	-	-	-	-

747 Online Methods

748 **Quality Control.** The 22 individual GWA studies were subjected to pre-established quality
749 control (QC) protocols as recommended elsewhere^{76,77}. Differences in genotyping chips, DNA
750 quality and genotype calling pipelines necessitated that QC parameters were tuned separately
751 to be appropriate for each individual study. At a minimum, we excluded markers with
752 excessively high missingness rates (> 5%), low minor allele frequency (< 1%), and failing a test
753 of Hardy-Weinberg equilibrium. We also excluded individuals with a high proportion of missing
754 genotypes (> 5%) and used identity-by-descent (IBD) estimates to remove individuals that were
755 highly related (IBD>0.185) to others in the sample. A summary of the genotyping platforms,
756 quality control, imputation protocols and association analysis methods used in each individual
757 GWA study is provided in **Supplementary Table 3**. All case/control sets that were genotyped
758 separately were first quality controlled independently and then again after merging the data.

759

760 To control for population stratification within each individual GWA study, we merged the
761 genotypes passing quality control filters with HapMap III genotype data from three populations;
762 European (CEU), Asian (CHB + JPT) and African (YRI). We then performed a principal
763 components analysis on the merged dataset and excluded any (non-European) population
764 outliers from our studies. To control for any further (sub-European) population structure, we
765 performed a second principal components analysis on the genotype data from each GWA study
766 separately to ensure that cases and controls were clustering together. We then tested whether
767 any principal components were significantly associated with the phenotype using logistic
768 regression. Any principal components that were significantly associated were then included as
769 covariates in the model when generating the final association test statistics for the migraine
770 meta-analysis. The specific principal components adjusted for in each individual GWA study are
771 listed in **Supplementary Table 4**.

772

773 **Imputation.** Following GWA study-level QC, the data underwent a phasing step whereby
774 haplotypes for each individual were statistically estimated using (in most instances) the program
775 SHAPEIT⁷⁸. Missing genotypes were then imputed into these haplotypes using the program
776 IMPUTE2⁷⁹ and a mixed-population reference panel provided by the 1000 Genomes Project¹⁶.
777 All study samples were imputed using the March 2012 (phase I, v3 release or later) 1000
778 Genomes reference panel. A minority of contributing GWA studies used alternative programs for
779 phasing and imputation such as BEAGLE⁸⁰, MACH⁸¹, and MINIMAC⁸² or some in-house custom
780 software. A full list of software and procedures used are provided in **Supplementary Table 3**.

781
782 **Statistical Analysis.** Individual study association analyses were implemented using logistic
783 regression with an additive model on the imputed dosage of the effect allele. All models were
784 adjusted for sex and other relevant covariates. Age information was not available for individuals
785 from all studies therefore we were not able to adjust for it in our models. However, we note that
786 all of the GWA studies were comprised of adults past the typical age of onset, hence age is at
787 most a non-confounding factor and false positive rates would not be affected by its
788 inclusion/exclusion. Furthermore, including such covariates can be sub-optimal, reducing power
789 to detect genetic associations. To control for sub-European population structure, we also
790 included in the model any principal components that were significantly associated with the
791 phenotype (**Supplementary Table 4**). The programs used for performing the association
792 analyses were either SNPTEST, PLINK or R (see URLs). To combine association summary
793 statistics from all individual studies we used the program GWAMA (URLs) to perform a fixed-
794 effects meta-analysis weighted by the inverse variance to obtain a combined effect size,
795 standard error and p-value at each marker. We excluded markers in any individual study that
796 had low imputation quality scores (IMPUTE2 *INFO* < 0.6 or MACH r^2 < 0.6) or low minor allele
797 frequency (MAF < 0.01). Additionally, we filtered out any marker that was missing from more
798 than half the individual studies (missing from 12 or more out of 22 studies) and also markers
799 exhibiting high levels of heterogeneity as identified by a high heterogeneity index (I^2 > 0.75).
800 After applying all filters, this left 8,045,569 total markers tested in the meta-analysis.

801
802 **Chromosome X meta-analysis.** Due to the different ploidy of males and females, the X
803 chromosome required a different statistical model; we applied a model of X-chromosome
804 inactivation (XCI) that assumes an equal effect of alleles in both males and females. This XCI
805 model was achieved by scaling male dosages to the range 0-2 to match that of females. In total,
806 57,756 cases and 299,109 controls were available for the X-chromosome analysis
807 (**Supplementary Table 1**). The reduced sample size compared to the autosomal data occurred
808 because some of the individual GWA studies (EGCUT, Rotterdam III, Twins UK, and 846
809 controls from GSK for the 'German MO' study) did not contribute chromosome X data.

810
811 **Defining Credible Sets.** Within each migraine-associated locus, we defined a credible set of
812 variants that could be considered 99% likely to contain a causal variant. The method has been
813 introduced in detail elsewhere^{52,58} and a full derivation is outlined again briefly in the
814 Supplementary Note. This method assumes that there is one and only one causal variant in the

815 locus. For loci that contain a secondary independent signal, we conservatively mapped only the
816 primary signal.

817

818 **LD score regression analysis.** We conducted a univariate heritability analysis based on
819 summary statistics using LD score regression (LDSC) v1.0.0⁵⁵. For this analysis, high-quality
820 common SNPs were extracted from the summary statistics by filtering the data using the
821 following criteria: presence among the HapMap Project Phase 3 SNPs⁸³, allele matching to
822 1000 Genomes data, no strand ambiguity, INFO score > 0.9, MAF >= 1%, and missingness less
823 than two thirds of the 90th percentile of total sample size. The HLA region (chromosome 6, from
824 25 - 35 Mb) was excluded from the analysis. From this data, we used LDSC to quantify the
825 proportion of the total inflation in chi-square statistics that can be ascribed to polygenic
826 heritability by calculating the ratio of the LDSC intercept estimate and the chi-square mean
827 using the formula described in the original publication⁵⁵.

828

829 **eQTL Credible Set Overlap Analysis.** To test whether the association statistics across each of
830 the 38 migraine loci could be explained by credible overlapping eQTL signals, we used two
831 previously published eQTL microarray datasets. The first dataset consisted of 3,754 samples
832 from peripheral venous blood⁸⁴ and the second was from a meta-analysis of human brain cortex
833 studies of 550 samples⁸⁵. From both studies we obtained summary statistics from an
834 association test of putative cis-eQTLs between all SNP-transcript pairs within a 1-Mb window of
835 each other. To test for overlapping eQTLs, we used credible sets of markers (see **Defining**
836 **Credible Sets**) at each of the 38 distinct migraine loci. Then for the most significant eQTLs ($P <$
837 1×10^{-4}) found to genes within a 1Mb window of each migraine credible set, we created an
838 additional credible set of markers for each eQTL. We then tested (using Spearman's rank
839 correlation) whether there was a significant correlation between the association test-statistics in
840 each migraine credible set compared to the expression test-statistics in each overlapping eQTL
841 credible set. Significant correlation between a migraine credible set and an eQTL credible set
842 was taken as evidence of the migraine locus tagging a real eQTL. We determined the
843 significance threshold to account for multiple testing by Bonferroni correction.

844

845 **Enhancer Enrichment Analysis.** Markers of gene regulation were defined using ChIP-seq
846 datasets produced at the Broad Institute and the University of California at San Diego as part of
847 ENCODE⁶⁵ and the NIH Roadmap Epigenome⁶⁴ projects. Based on the histone H3K27ac
848 signal, which identifies active enhancers, we processed data from 56 cell lines and tissue

849 samples to identify celltype- or tissue-specific enhancers, which we define as the 10% of
850 enhancers with the highest ratio of reads in that cell or tissue type divided by the total reads⁸⁶. A
851 description of all 56 tissues/cell types is provided in **Supplementary Table 21** and the raw
852 enhancer data can be downloaded at <http://www.epigenomeatlas.org>.

853
854 We mapped the candidate causal variants at each migraine associated locus to these enhancer
855 sequences, and compared the overlap observed with tissue specific enhancers relative to all
856 enhancers using a background of 10,000 randomly selected sets of SNPs of equal size as the
857 original locus. We restricted the background selection to common variants (MAF>1%) from
858 1000 Genomes that also passed our quality control filters in the meta-analysis (in other words,
859 to only allow the selection of SNPs that had an *a priori* chance of being associated). The
860 selection procedure then involved randomly selecting regions of the genome that were of
861 equivalent length and containing an equivalent density of enhancers as found in the original
862 locus. Once an appropriate region was found, a set of SNPs was randomly selected to match
863 the number of SNPs in the credible set for that locus. If the selected SNPs happened to fall in
864 an equal number of enhancer sites (of any tissue type) as that of the credible set of SNPs from
865 the original locus, then the selected set of SNPs was accepted and added to the background set
866 of SNPs for comparison. If the number of enhancers overlapping with the selected SNPs didn't
867 match, the randomized selection procedure was repeated until an appropriate comparison set of
868 SNPs was selected. This selection procedure was repeated for each locus 10,000 times to
869 obtain an empirical null distribution. The significance of the observed enrichment was then
870 estimated from the empirical distribution by calculating the proportion of replicates that were
871 greater than the observed value (i.e. *Empirical P-value* = $[R + 1]/[N + 1]$ where R is the number
872 out of all N replicates that were higher than the observed enrichment). Finally, we used
873 Bonferroni correction to adjust for multiple testing of 56 tissue/cell types ($P < 8.9 \times 10^{-4}$).

874
875 **DEPICT reconstituted gene-set enrichment analysis.** DEPICT⁶² (Data-driven Expression
876 Prioritized Integration for Complex Traits) is a computational tool, which, given a set of GWAS
877 summary statistics, allows prioritization of genes in associated loci, enrichment analysis of
878 reconstituted gene sets, and tissue enrichment analysis. DEPICT was run using as input 124
879 independent genome-wide significant SNPs (PLINK clumping parameters: --clump-p1 5e-8 --
880 clump-p2 1e-5 --clump-r2 0.6 --clump-kb 250. Note - rs12845494 and rs140002913 could not be
881 mapped). LD distance ($r^2 > 0.5$) was used to define locus boundaries (note that this locus
882 definition is different than used elsewhere in the text) yielding 37 autosomal loci comprising 78

883 genes. DEPICT was run using default settings, that is, 500 permutations for bias adjustment, 20
884 replications for false discovery rate estimation, normalized expression data from 77,840
885 Affymetrix microarrays for gene set reconstitution (see reference⁸⁷), 14,461 reconstituted gene
886 sets for gene set enrichment analysis, and testing 209 tissue/cell types assembled from 37,427
887 Affymetrix U133 Plus 2.0 Array samples for enrichment in tissue/cell type expression.

888

889 DEPICT identified 76 reconstituted gene sets that are significantly enriched ($FDR < 5\%$) for
890 genes found among the 38 migraine associated loci. Post-analysis, we omitted reconstituted
891 gene sets in which genes in the original gene set were not nominally enriched (Wilcoxon rank-
892 sum test) because, by design, genes in the original gene set are expected to be enriched in the
893 reconstituted gene set; lack of enrichment therefore complicates interpretation of the
894 reconstituted gene set because the label of the reconstituted gene set will be inaccurate.
895 Therefore the following reconstituted gene sets were removed from the results (Wilcoxon rank-
896 sum P -values in parentheses): MP:0002089 (0.01), MP:0002190 (0.16), ENSG00000151577
897 (0.21), ENSG00000168615 (0.94), ENSG00000143322 (0.70), ENSG00000112531 (0.04),
898 ENSG00000161021 (0.10), ENSG00000100320 (0.43). We also removed an association
899 identified to another gene set (ENSG00000056345 PPI, $P = 1.7 \times 10^{-4}$, $FDR = 0.04$) because it is
900 no longer part of the Ensembl database. These post-analysis filtering steps left us with 67
901 significantly enriched reconstituted gene sets. The Affinity Propagation tool⁸⁸ was finally used to
902 cluster related reconstituted gene sets into 10 groups (script to produce the network diagram
903 can be downloaded from <https://github.com/perslab/DEPICT>).

904

905 **DEPICT tissue enrichment analysis.** For the tissue enrichment analysis, DEPICT incorporates
906 data from 37,427 human microarray samples captured on the Affymetrix HGU133a2.0 platform.
907 These are used to test whether genes in the 38 migraine loci are highly expressed in 209
908 tissues/cell types with Medical Subject Heading (MeSH) annotations. The annotation procedure
909 and method for normalizing expression profiles across annotations is outlined in the original
910 publication⁶². The tissue/cell type enrichment analysis algorithm is conceptually identical to the
911 gene set enrichment analysis algorithm whereby enrichment P -values are calculated empirically
912 using 500 permutations for bias adjustment and 20 replications for false discovery rate
913 estimation.

914

915 **GTEX tissue enrichment analysis.** Credible sets were generated for all 38 migraine loci (with
916 $P < 5 \times 10^{-8}$) and corresponding gene sets for each locus were then generated by taking all

917 genes within 50 kilobases of a credible set SNP. Genes identified in this way were then
918 analyzed for tissue enrichment using publicly available expression data from pilot phase of the
919 Genotype-Tissue Expression project (GTEx)⁶¹, version 3. In the pilot phase dataset, *postmortem*
920 samples from 42 human tissues and three cell lines across 1,641 samples (**Supplementary**
921 **Table 16**) have been used for bulk RNA sequencing according to a unified protocol. All samples
922 were sequenced using Illumina 76 base-pair paired-end reads.

923

924 Collapsed reads per kilobase per million mapped reads (RPKM) values for each of the 52,577
925 included transcripts, filtered for unique HGNC IDs ($n = 20,932$), were organized by tissue and
926 individual ($n_{tissues} = 45$, $n_{samples} = 1,641$). By this process we also excluded transcripts from any
927 non-coding RNAs. All transcripts were ranked by mean RPKM across all samples, and 100,000
928 permutations of each credible set gene list were generated by selecting a random transcript for
929 each entry in the credible set within +/-100 ranks of the transcript for that gene. For each
930 sample, the RPKM values were converted into ranks for that transcript, and sums of ranks
931 within each tissue were computed for each gene. *P*-values for each tissue were calculated by
932 taking the total number of cases where the gene list of interest had a lower sum of ranks than
933 the permuted sum of ranks, and dividing by the total number of permutations. To assess the
934 significance of the enrichment after testing multiple tissues, we used a Bonferroni correction
935 adjusted for the number of independent tissues, estimated via the matSpD tool⁸⁹ to arrive at 27
936 independent tests and a significance threshold of $P < 1.90 \times 10^{-3}$.

937

938 **Specificity of individual gene expression in GTEx tissues.** For the individual-gene
939 expression analysis, we selected the closest gene to the index SNP at each migraine locus and
940 then investigated expression activity of each of these genes in the collection of available
941 tissues. As the number of samples for some tissues was small, we grouped individual tissues
942 into four categories; brain, vascular, gastrointestinal, and other tissues (**Supplementary Table**
943 **16**). Then for each selected gene, we tested whether the average expression (mean RPKM)
944 was significantly higher in a particular tissue group compared to the “other tissues” category.
945 We assessed significance using a one-tailed t-test and used Bonferroni correction to control for
946 multiple testing for all 114 tests (38 genes \times 3 tissue groups). While some genes were observed
947 to be significantly expressed in multiple tissue groups, we determined that a gene was tissue-
948 specific if it was only expressed highly in one tissue group (i.e. brain, vascular, or
949 gastrointestinal, **Supplementary Table 25**).

950

951 **eQTL credible set analysis in GTEx tissues.** For all tissues and transcripts, we identified
952 genome-wide significant ($P < 2 \times 10^{-13}$) *cis*-eQTLs within a 1Mb window of each transcript and
953 created credible sets (see **Defining Credible Sets**) for each eQTL locus identified in each
954 tissue. Then, for each eQTL credible set that contained markers that overlapped with a migraine
955 credible set, we tested using Spearman's rank correlation if the test statistics between the two
956 overlapping credible sets were significantly correlated. Significant correlation between a
957 migraine credible set and an eQTL credible set was taken as evidence of the migraine locus
958 tagging a real eQTL. Multiple testing was controlled for using Bonferroni correction.

959

960 Across the GTEx collection of tissues we found 35 significant *cis*-eQTLs within a 1Mb window of
961 the 38 migraine loci, however, upon creating credible sets, seven of these still contained SNPs
962 that overlapped with any of the migraine credible sets. Testing these seven eQTL credible sets
963 as described above found that the correlation was significant ($P < 7.1 \times 10^{-3}$) for eQTLs to four
964 tissues (Lung, Thyroid, Tibial Artery, and Aorta) at two migraine loci (*HPSE2* and *HEY2*)
965 **Supplementary Table 19** and **Supplementary Figure 15**.

966

967 **Heterogeneity analysis of migraine subtypes.** To discover if heterogeneity between the
968 migraine subtypes might have affected our ability to identify new loci, we performed an
969 additional meta-analysis using a subtype-differentiated approach that allows for different allelic
970 effects between the two groups⁵⁷. Since a large proportion of the controls were shared in the
971 original migraine with aura and migraine without aura samples (see **Table 1**), for this analysis
972 we created two additional subsets of the migraine subtype data that contained no overlapping
973 controls between the two new subsets (**Supplementary Table 12**). The new migraine with aura
974 subset consisted of 4,837 cases and 49,174 controls and the new migraine without aura subset
975 consisted of 4,833 cases and 106,834 controls. Then using the association test statistics from
976 each of the individual GWA studies listed, we performed the subtype-differentiated meta-
977 analysis as implemented in GWAMA (see URLs).

978

979 To assess the amount of heterogeneity observed, we chose the 44 LD independent SNPs that
980 were associated with migraine and examined the results of the subtype-differentiated meta-
981 analysis. We observed that only seven out of the 44 SNPs showed evidence for heterogeneity
982 in the subtype-differentiated test (Heterogeneity P -value < 0.05 , **Supplementary Table 13**).
983 This suggests that most of the identified loci are truly affecting risk for both migraine with aura

984 and migraine without aura even though we may not yet have power to detect their association in
985 the subset meta-analyses.
986

987 **Methods references**

- 988 76. Anderson, C. A. *et al.* Data quality control in genetic case-control association studies.
989 *Nat. Protoc.* **5**, 1564–1573 (2010).
- 990 77. Winkler, T. W. *et al.* Quality control and conduct of genome-wide association meta-
991 analyses. *Nat. Protoc.* **9**, 1192–1212 (2014).
- 992 78. Delaneau, O., Marchini, J. & Zagury, J.-F. A linear complexity phasing method for
993 thousands of genomes. *Nature Methods* **9**, 179–181 (2011).
- 994 79. Howie, B., Fuchsberger, C., Stephens, M., Marchini, J. & Abecasis, G. R. Fast and
995 accurate genotype imputation in genome-wide association studies through pre-phasing.
996 *Nature Genetics* **44**, 955–959 (2012).
- 997 80. Browning, S. R. & Browning, B. L. Rapid and accurate haplotype phasing and missing-
998 data inference for whole-genome association studies by use of localized haplotype
999 clustering. *Am. J. Hum. Genet.* **81**, 1084–1097 (2007).
- 1000 81. Li, Y., Willer, C. J., Ding, J., Scheet, P. & Abecasis, G. R. MaCH: Using sequence and
1001 genotype data to estimate haplotypes and unobserved genotypes. *Genet. Epidemiol.* **34**,
1002 816–834 (2010).
- 1003 82. Fuchsberger, C., Abecasis, G. R. & Hinds, D. A. minimac2: faster genotype imputation.
1004 *Bioinformatics* **31**, 782–784 (2015).
- 1005 83. The International HapMap 3 Consortium. Integrating common and rare genetic variation
1006 in diverse human populations. *Nature* **467**, 52–58 (2010).
- 1007 84. Wright, F. a *et al.* Heritability and genomics of gene expression in peripheral blood. *Nat.*
1008 *Genet.* **46**, 430–7 (2014).
- 1009 85. Richards, A. L. *et al.* Schizophrenia susceptibility alleles are enriched for alleles that
1010 affect gene expression in adult human brain. *Mol. Psychiatry* **17**, 193–201 (2012).
- 1011 86. Farh, K. K.-H. *et al.* Genetic and epigenetic fine mapping of causal autoimmune disease
1012 variants. *Nature* **518**, 337–343 (2014).
- 1013 87. Fehrmann, R. S. N. *et al.* Gene expression analysis identifies global gene dosage
1014 sensitivity in cancer. *Nat. Genet.* **47**, 115–125 (2015).
- 1015 88. Frey, B. J. & Dueck, D. Clustering by Passing Messages Between Data Points. *Science*
1016 *(80-)*. **315**, 972–976 (2007).
- 1017 89. Nyholt, D. R. A simple correction for multiple testing for single-nucleotide polymorphisms
1018 in linkage disequilibrium with each other. *Am. J. Hum. Genet.* **74**, 765–769 (2004).